

Review

# Development Trends of Internal Inspection Equipment and Technologies for Long-Distance Oil and Gas Pipelines

Bin Liu<sup>1</sup>, Zheng Lian<sup>1\*</sup>, Ye Tian<sup>2</sup>, Xinyang Dong<sup>1</sup>, Rongxue Li<sup>1</sup>, Luyao He<sup>1</sup>, Meng Li<sup>1</sup>, Lijian Yang<sup>1</sup>

<sup>1</sup> School of Information Science and Engineering, Shenyang University of Technology, Shenyang, Liaoning Province, China

<sup>2</sup> United Pipeline Co., Ltd., Pipe Network Group (Xinjiang), Urumqi, Xinjiang Uygur Autonomous Region, China

\* Corresponding author email: [lianzhengsut@smail.sut.edu.cn](mailto:lianzhengsut@smail.sut.edu.cn)

**Abstract:** As critical national infrastructure, oil and gas pipelines are hailed as "energy arteries". In-line inspection (ILI) is internationally recognized as the most effective method for pipeline safety maintenance. This paper sorts out and compares the current mainstream pipeline ILI technology systems, including diameter variation, Magnetic Flux Leakage (MFL), weak magnetic, dual magnetic field, eddy current, balanced electromagnetic, piezoelectric ultrasonic, and electromagnetic ultrasonic technologies, covering mainstream pipeline damage types such as geometric deformation, corrosion, wall thinning, stress concentration areas, composite defects, surface and near-surface cracks, buried microcracks, and weld cracks. Among them, diameter variation detectors mainly target pipeline geometric deformation and are mostly used for passability auxiliary judgment before ILI construction; MFL detection features fast speed, high sensitivity, mature theory, and strong penetration, enabling efficient detection of macro volume defects such as corrosion; weak magnetic and dual magnetic field technologies can identify stress concentration areas, but MFL, weak magnetic, and dual magnetic field methods are only applicable to ferromagnetic materials, and the quantitative relationship between magnetic signals and defects needs further improvement; eddy current and balanced electromagnetic methods excel in high-precision detection of surface and near-surface cracks in conductive materials with relatively fast detection speed, and the current core challenges are enhancing deep defect penetration capability and reducing the interference of lift-off value on signals; piezoelectric ultrasonic and electromagnetic ultrasonic technologies have a wide material adaptation range and high detection precision, and can assist in identifying composite defects and weld cracks. However, piezoelectric ultrasonic relies on couplants, has strict requirements on the flatness of the detection environment, and relatively low detection speed. The current key challenge lies in improving the signal-to-noise ratio through signal processing. Based on different principles, various technologies form a complement to each other, jointly constructing a detection system with wide coverage and strong adaptability. By elaborating on the principles, performance characteristics, application scenarios, and domestic and foreign research trends of each technology, this paper clarifies the positioning and advantages of different technologies in pipeline damage detection, providing clear technical selection references for pipeline safety maintenance personnel and helping to improve the scientificity and efficiency of oil and gas pipeline safety operation and maintenance.

**Keywords:** pipeline in-line inspection; magnetic flux leakage; electromagnetic ultrasonic testing; eddy current testing; pipeline integrity assessment



**Copyright:** © 2026 by the authors. This article is licensed under a Creative Commons Attribution 4.0 International License (CC BY) license (<https://creativecommons.org/licenses/by/4.0/>).

**Citation:** Bin Liu, Zheng Lian, Ye Tian, Xinyang Dong, Rongxue Li, Luyao He, Meng Li, Lijian Yang. "Development Trends of Internal Inspection Equipment and Technologies for Long-Distance Oil and Gas Pipelines." *Instrumentation* 13, no.1 (March 2026). <https://doi.org/10.15878/j.instr.202600359>

# 1 Introduction

Pipeline transportation is one of the main international oil and gas transportation methods. Since the world's first oil pipeline was built in Pennsylvania, USA in 1865, the pipeline transportation industry has a history of more than 100 years<sup>[1-3]</sup>. According to the statistics of the CIA World Factbook, the total length of global oil and gas pipelines is about 2.019 million kilometers, including 1.35 million kilometers of natural gas pipelines, accounting for 66.9% of the total pipeline length; 401,000 kilometers of crude oil pipelines, accounting for 19.8%; and 268,000 kilometers of product oil pipelines, accounting for 13.3%<sup>[4,5]</sup>. Currently, 99% of natural gas and 70% of oil in China's land are transported by pipelines. According to the Energy Data Handbook of CNPC Economics & Technology Research Institute, by the end of 2024, the total length of China's oil and gas pipelines has increased from 24,660 kilometers in 2000 to an estimated 191,500 kilometers. Among them, the length of crude oil pipelines has grown from 11,201 kilometers in 2000 to 32,000 kilometers in 2024; the length of natural gas pipelines has increased from 12,262 kilometers in 2000 to 127,500 kilometers in 2024; and the length of product oil pipelines has risen from 1,197 kilometers in 2000 to 32,000 kilometers in 2024, covering dozens of provinces, cities and municipalities nationwide as well as vast sea areas such as the Bohai Sea, the Yellow Sea, and the South China Sea. It is estimated that the total length will reach 240,000 kilometers by the end of 2025. Oil and gas pipelines are the lifeline for national economic development and people's livelihood security<sup>[6]</sup>. In addition, China's energy consumption will maintain rapid growth from 2020 to 2030. It is expected that the natural gas demand will reach 526 billion cubic meters by 2030 and peak at 650 billion cubic meters by 2035. Compared with the current consumption level, the demand increment will be 200-320 billion cubic meters, which will drive the accelerated construction of infrastructure such as oil and gas pipeline networks<sup>[7-9]</sup>.

With the gradual advancement of China's hydrogen energy strategic layout and the proposal of the "carbon neutrality and carbon peaking" vision, new energy transmission pipelines such as hydrogen transmission pipelines and CO<sub>2</sub> transportation pipelines have emerged rapidly, providing key support for energy structure transformation. Academician Huang Weihe pointed out that the construction of long-distance CO<sub>2</sub> pipelines and their supporting infrastructure is a necessary condition for China to achieve the carbon neutrality vision<sup>[10]</sup>. However, the development of new pipelines combined with the operation and maintenance of existing pipelines has brought multiple severe challenges to China's pipeline safety maintenance. At the level of existing pipelines, most of China's pipelines have been in service for more than 20 years, and many macro volume defects

have been formed due to material aging, corrosion, fatigue and other factors. These defects pose significant hidden dangers to the safe operation of pipelines. For example, the Qingdao 11·22 accident resulted in 62 deaths, 136 injuries, and direct economic losses of 750 million yuan<sup>[11]</sup>. At the level of new pipelines, with the acceleration of China's pipeline construction, various stresses such as pipeline welding residual stress, heat treatment residual stress, assembly stress, and construction damage have increased sharply; the combined effect of these stresses and the pipeline service environment will cause hydrogen-induced cracking, corrosion cracking, etc., which will further lead to brittle fracture of pipelines, resulting in heavy casualties and economic losses<sup>[12,13]</sup>. Pipeline accidents caused by stress damage have attracted great attention from the domestic and foreign pipeline industries. Statistical results show that 17.3% of accidents are sudden pipe bursts caused by stress concentration. At this time, no volume defects are formed, which are highly concealed, and their detection has become an "international problem"<sup>[14]</sup>. At the risk level brought by new transmission media, when macro defects coexist with stress concentration areas, the danger is the highest. Stress will accelerate the expansion of macro defects, and defects will amplify stress concentration, forming a vicious circle. It is not only difficult to distinguish the main cause of failure and identify stress, but also greatly shorten the failure time, which is very easy to cause sudden pipeline burst, becoming the most harmful and difficult-to-deal-with threat to pipelines.

To address these complex and hidden pipeline risks, advanced non-destructive testing technologies are urgently required—with high-end sensors as the core cornerstone. As Academician You Z<sup>[15]</sup> emphasized, sensors serve as the "bridge" connecting the physical and digital worlds, and their performance directly dictates the detection capability of key equipment. Against this backdrop, in-line inspection (ILI) has emerged as the internationally recognized most effective pipeline operation and maintenance method<sup>[16]</sup>. Pipeline inspection gauges (PIGs) traverse pipelines driven by transmission media (operating speed: 1m/s ~ 5m/s; continuous operation mileage: > 100km), enabling on-line non-destructive testing for deformation, corrosion, cracks, and stress concentration. With advantages of high efficiency and non-contact operation, PIGs provide a scientific basis for pipeline operation, maintenance, and safety evaluation.

Globally, a preliminary ILI standard system has taken shape, covering technical requirements for detection implementation, equipment performance, and result evaluation. Domestically, standards such as GB/T 27699-2023<sup>[17]</sup> and SY/T 6597-2018<sup>[18]</sup> specify detailed requirements for geometric deformation, metal loss, and other key detection items for steel pipelines. Internationally, specifications including POF 100<sup>[19]</sup> and

NACE 35100<sup>[20]</sup> focus on unifying detection process norms and equipment performance verification criteria,

laying a standardized foundation for global pipeline ILI practices.

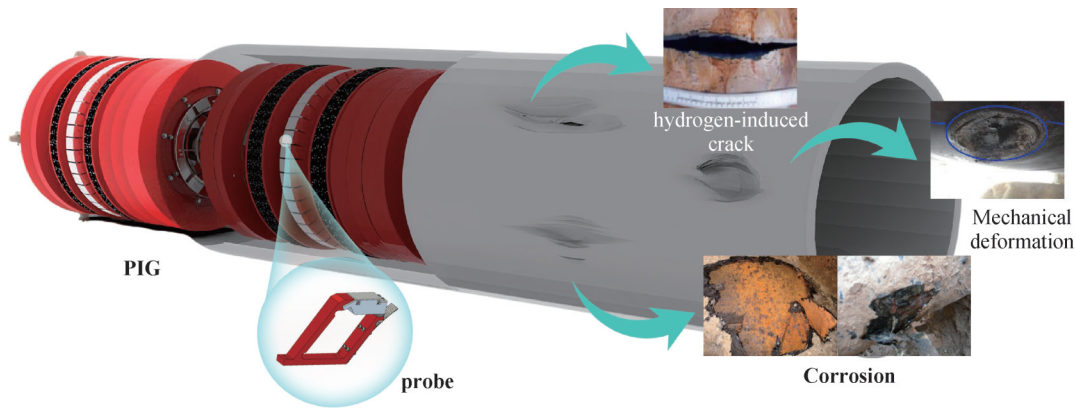


Fig.1 Oil and Gas Pipeline ILI Technology

In response to complex pipeline defect types, ILI technology has been continuously iterated, deriving various detection methods such as geometry inspection, Magnetic Flux Leakage (MFL), Low Field Magnetic Flux Leakage (LMFL), Dual Magnetic Field (DMG), Eddy Current Testing (ECT), Balanced-field Electromagnetic

(BE), Piezoelectric Ultrasonic Testing (PZT-UT), and Electromagnetic Acoustic Transducer (EMAT). Emerging composite ILI methods are also gradually developing. The application scenarios of each detection method are compared as shown in Table 1.

Table 1 Current Mainstream Oil and Gas Pipeline ILI Technologies

Detection Method	Applicable Materials	Defect Detection Types	Detection Speed	Typical Application Scenarios
Geometry	Various materials	Dents, elliptical deformation, wall thickness changes, and various pipeline accessories causing changes in pipeline inner diameter	High	Usually used for diameter measurement of new pipelines and passability determination before pipeline internal inspection
MFL <sup>[21]</sup>	Ferromagnetic materials	Volume defects (corrosion, wall thinning)	High	Rapid screening of long-distance crude oil and product oil pipelines
LMFL <sup>[22]</sup>	Ferromagnetic materials	Potential defects such as stress concentration areas	High	Auxiliary detection for early warning of pipeline defects
DMG <sup>[23]</sup>	Ferromagnetic materials	Volume defects and stress concentration areas	High	Pipeline detection with coexistence of complex stress and volume defects
ECT <sup>[24]</sup>	Conductive materials	Surface and near-surface defects (cracks, corrosion)	Medium	Rapid detection of pipeline welds, surface defects, and cracks
BE <sup>[25]</sup>	Conductive materials	Surface, near-surface, and buried defects (cracks, corrosion)	Medium	Scenarios requiring high-precision detection of internal defects and cracks
UT <sup>[26]</sup>	Various materials	Various defects (quantification of depth and shape)	Low	Crack detection of oil transmission pipelines
EMAT <sup>[27, 28]</sup>	Various materials	Various defects (special working conditions)	Low	Crack detection of various pipelines

It can be seen from the comparison in Table 1 that in terms of applicable materials, methods relying on material magnetic properties such as MFL, LMFL, and DMG are only applicable to ferromagnetic materials (such as X80, X70, Q235 pipes); methods such as ECT and BE have a wider application range, covering the above ferromagnetic materials as well as conductive materials; UT and EMAT are applicable to pipelines of all materials. However, since UT relies on coupling media, it is suitable for liquid transmission pipelines, while EMAT

is theoretically applicable to both oil and gas transmission pipelines.

In terms of detected defect types, MFL is mainly used to identify volume defects such as metal loss and corrosion; LMFL focuses on early warning of stress damage; and DMG, as a composite detection technology, can evaluate the stress concentration level of composite defects; ECT is suitable for detection of surface and near-surface open cracks; BE covers detection of buried internal microcracks; UT and EMAT are mainly aimed at

detection of surface and internal cracks.

From the perspective of market application, corrosion detection accounts for 45% of the global pipeline ILI market. The MFL-PIG has a relatively simple structure, no need for complex coupling media, a long maintenance cycle, and a clear physical mechanism of defect response, making MFL the current mainstream ILI technology. As a key factor causing major pipeline accidents, the demand for crack detection continues to grow with a compound annual growth rate of 2.9%, driving the accelerated application of crack detection technology in preventive maintenance and forming a market pattern complementary to MFL<sup>[29]</sup>.

These characteristics together constitute a diversified pipeline ILI system, which can meet the defect detection needs in different scenarios. Based on this, this paper systematically sorts out the ILI technologies for long-distance oil and gas pipelines, compares the characteristics of mainstream methods, analyzes the development progress of emerging composite detection technologies, and puts forward prospects for future technical directions, providing references for the research and practice of pipeline safety operation and maintenance.

## 2 Oil and Gas Pipeline Geometry ILI Technology

The oil and gas pipeline geometry PIG is a detection device targeting abnormal pipeline geometric parameters. It is mainly used to detect pipeline dents, elliptical deformation, wall thickness changes, and various pipeline

accessories causing changes in pipeline inner diameter. It can also identify pipeline features and deformation such as straight pipe sections, elbows, mileage, tees, miter joints, and welds. Its basic detection principle is to adopt micro-electromagnetic technology combined with a mechanical arm structure to realize the detection of pipeline geometric deformation, and it has a strong ability to pass through pipeline deformations, being able to safely pass through pipeline deformation sections with a deformation amount of 25%. With technological upgrading, the new generation of geometry detectors can be equipped with an Inertial Measurement Unit (IMU) to further realize the detection of pipeline centerline trajectory and direction.

In terms of the application scenarios of oil and gas pipeline geometry ILI technology, it mainly covers various key working conditions: when the caliper plate of the caliper pig is severely deformed and the accurate position of the deformation point cannot be determined, the detector is needed to clarify the defect position; before the new pipeline is put into trial operation, it is necessary to complete the geometric parameter detection during the acceptance stage with its help; if the in-service pipeline is subjected to long-term occupation by overloaded objects or mechanical damage, or natural disasters such as debris flow and landslides occur in the passing area, as well as earthquakes above magnitude 5 on the Richter scale, the detector is required to check the deformation risk; in addition, in the pipeline safety assessment work, the detector can be used as a special detection method to support the assessment needs. The current mainstream geometry PIGs are shown in Figure 2.

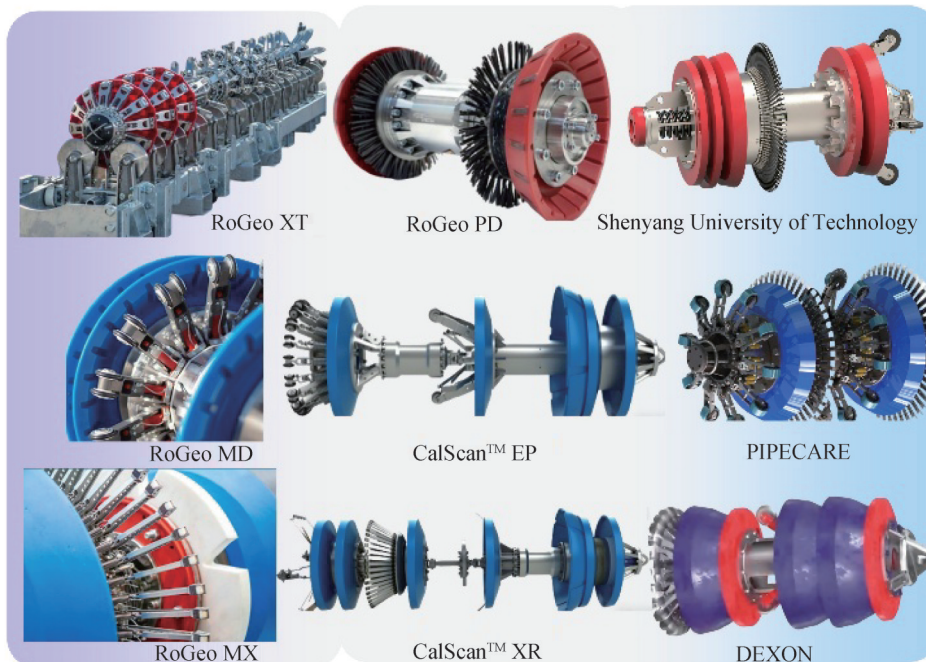


Fig.2 Current Mainstream Geometry PIGs(RoGeo XT, RoGeo PD, Shenyang University of Technology, RoGeo MD, CalScan EP, PIPECARE, RoGeo MX, CalScan XR, RoGeo MX, DEXON)

In addition to the above scenarios, the geometry detector also plays a pre-protection role in the MFL ILI process. Since the MFL-PIG needs to magnetize the pipe wall through built-in yokes, permanent magnets, and steel brushes, and needs to be close to the inner pipe wall to ensure effective magnetization, its pipeline passing ability is weak. If it is directly put into operation without clarifying the pipeline deformation, it may cause safety accidents such as equipment jamming and damage. Therefore, before carrying out MFL ILI, it is necessary to first put into operation the geometry detector to find out the pipeline deformation status, so as to ensure the safe and efficient operation of MFL ILI.

From the perspective of the current industry technology, since it is generally used as a pre-project for MFL ILI construction, most international mainstream internal inspection companies currently have mature diameter variation detection capabilities. Representative products include the butterfly cup deformation internal detector developed by GE PII of the United States, and the MultiDiameter high-passability deformation internal detector of Rosen of Germany. At the same time, many internal inspection companies have similar products. The core performance indicators of these products are basically the same, jointly forming the current technical application pattern. The performance index parameters of current mainstream geometry PIGs are compared as shown in Table 2.

As can be seen from Table 2, many companies currently have geometry detection capabilities. Among them, Rosen of Germany has a wide variety of geometry PIGs, including RoGeo MD, RoGeo MX, RoGeo XT (combining mechanical calipers with eddy current proximity sensors), as well as RoGeo PD (equipped with IMU) and RoGeo MHT (equipped with hysteresis loop sensors). Companies such as Baker Hughes (merged with PII) can also realize related functions with similar performance indicators.

In China, the Pipeline In-line Inspection Research Team at Shenyang University of Technology has been a significant contributor to the field since the 1990s. Supported by platforms such as the Liaoning Provincial Engineering Research Center for In-line Inspection of Long-Distance Oil and Gas Pipelines and the Liaoning Provincial Key Laboratory of In-line Inspection for Oil and Gas Pipelines, the team has conducted extensive research and developed a series of engineering tools in areas including MFL, LMFL, and DMG technologies. Their work has been applied in major national projects such as the West-East Gas Pipeline and the China-Russia East-Route Pipeline, with cumulative service mileage exceeding 100,000 kilometers. The team has also actively participated in the formulation of industry standards, providing both theoretical and practical support for the advancement of domestic pipeline inspection capabilities<sup>[34]</sup>.

Against this backdrop, magnetic-based inspection

technologies (MFL, LMFL, DMG) have become the most widely adopted methods for pipeline defect assessment. The following section elaborates on their principles, equipment, and development trends.

### 3 Oil and Gas Pipeline MFL ILI Technology

The core principles of the three pipeline ILI technologies (MFL, LMFL, and DMG) all utilize the magnetic domain response characteristics of ferromagnetic materials under the action of a magnetic field. When there are defects or stress concentration in the pipeline, local magnetic field distortion will occur. Magnetic sensitive sensors capture these magnetic signal abnormalities to realize the identification and evaluation of pipeline damage. The basic principles of these pipeline ILI technologies are shown in Figure 3.

As can be seen from Figure 3, the core working principle of MFL technology is to apply a high-intensity magnetic field to the pipeline through permanent magnets to magnetize the pipeline material to a near-saturation state; when there are defects in the material, the magnetic permeability of the defect area will change abruptly, causing the magnetic induction lines originally uniformly distributed inside the material to leak along the defect contour; the detection equipment captures this magnetic induction line distortion signal through built-in probes, thereby realizing the identification and detection of pipeline defects. The core difference between MFL and LMFL mainly lies in the external excitation intensity, while DMG technology realizes the integration of their advantages. Among them, LMFL utilizes the characteristic that the magnetic domains of pipeline materials will move directionally in stress concentration areas, forming a weak magnetic field in that area; high-sensitivity magnetic sensors capture this magnetic field, which can identify the characteristics of early stress damage of pipelines, thereby realizing the detection of hidden stress damage. The DMG technology adopts a unique segmented excitation structure design: its front section adopts a strong excitation mode to simulate MFL working conditions, which can efficiently detect pipeline geometric defects; the rear section switches to a weak excitation environment to simulate LMFL working conditions, and accurately detects the stress state at the defect position by capturing the magnetic field abnormal signal in the stress concentration area. At present, the international mainstream detection equipment for MFL, LMFL, and DMG is shown in Figure 4.

Taking MFL-PIG as an example, this paper introduces the key components and functions of PIG, and reveals how each part supports the whole process of magnetic signal collection, equipment operation, and data integration. PIG mainly consists of three systems: probe, power drive (cup), and positioning calibration (mileage,

Table 2 Mainstream Geometry PIGs

Manufacturer/ Institution	Representative Product	Detection Threshold (POD=90%)		Detection Accuracy (Confidence=90%)		Dent Depth	Wall Thickness Change	Ellipticity	Dent Depth	Wall Thickness Change	Ellipticity	Dent Depth	Axial Positioning Accuracy	Circumferential Positioning Accuracy	Applicable Pipe Diameter	Detection Object	Detection Speed
		Wall Thickness Change	Ellipticity	Dent Depth	Wall Thickness Change												
NACE [20]	NACE 35100	1mm	1.0-3mm	3-5mm	±1.0mm	±1.0-3.0mm	±1.0-3.0mm	±1.0-3.0mm	±1.5% (≤219.1mm) ±1.0% (≥273mm) (Confidence=80%)	±1.0mm (weld)	±5.0°	88.9-1422mm	±15°	88.9-1422mm	Dents, wrinkles, bends, and fittings	≤5m/s	
ROSEN [30]	RoGeo MD	±1.5 mm	1.0%	1.0 %	±1.5 mm	1.0%	±1.5 mm	1.0%	±0.5 % (≤406.4mm) ±0.3 % (>406.4mm) (Confidence=80%)	±0.8 mm	1.0 %	±0.5 % (≤406.4mm) ±0.3 % (>406.4mm) (Confidence=80%)	Not marked	±15°	219, 1-1422mm	Ellipticity, dents, bulges, bends	≤5m/s
	RoGeo XT	±0.8 mm	0.5%	0.5%	±0.8 mm	0.5%	±0.8 mm	0.5%	±0.2 % (762-965.2mm) ±0.15 % (1016-1422mm) (Confidence=80%)	±0.8 mm	0.5%	±0.2 % (762-965.2mm) ±0.15 % (1016-1422mm) (Confidence=80%)	Not marked	±12°	168.3-1422mm	Ellipticity, dents, bulges, bends, and stress-induced features	≤5m/s
	CalScan™	Not marked	Not marked	Not marked	Not marked	Not marked	Not marked	Not marked	1.0 % (<273 mm) 0.8 % (273-406.4mm) 0.5 % (457-711mm) 0.3 % (762-965.2mm) 0.2 % (1016-1422mm) (POD=95%)	Not marked	Not marked	Not marked	Not marked	Not marked	Not marked	Geometric defects	Not marked
	CalScan™ EP	Not marked	Not marked	Not marked	Not marked	Not marked	Not marked	Not marked	Not marked	Not marked	Not marked	Not marked	Not marked	Not marked	Not marked	Not marked	Geometric, weld, and mapping detection
Baker Hughes (PII)	CalScan™ XR	Not marked	Not marked	Not marked	Not marked	Not marked	Not marked	Not marked	Not marked	Not marked	Not marked	Not marked	Not marked	Not marked	Not marked	Geometric defects (denser probe distribution)	Not marked
Dexon [31]	Caliper Pig	Not marked	Not marked	Not marked	Not marked	Not marked	Not marked	Not marked	Not marked	Not marked	Not marked	Not marked	Not marked	Not marked	114.3-1422mm	Dents, bulges, pipeline expansion, and buckling measurement	Not marked
PIPECARE [32]	Geometry pig	Not marked	2% (POD=95%)	Not marked	Not marked	Not marked	Not marked	Not marked	Not marked	Not marked	2%	1.5%	±/- 0.15 m (weld)	+/- 10°	Not marked	Dents, wrinkles, ellipticity, inner diameter changes	Not marked
Shenyang University of Technology [33]	Pipeline Geometry Internal Detector	1.5mm	1%	1% OD	±1mm	±1%	±2mm (OD≤406mm) ±3.5mm (406mm<OD<1016mm) ±5mm (OD≥1016mm)	±1%	±1*% (OD≥1016mm)	±1*% (OD≥1016mm)	±5.0°	Φ159-Φ1422mm	±5.0°	Φ159-Φ1422mm	thickness changes, and various pipeline accessories causing changes in pipeline inner diameter	≤5m/s	

OD = pipe outer diameter; Ellipticity (%) = (maximum diameter - minimum diameter)/nominal diameter; t = pipe wall thickness; POD = Probability of Detection; 1 = calibration point spacing

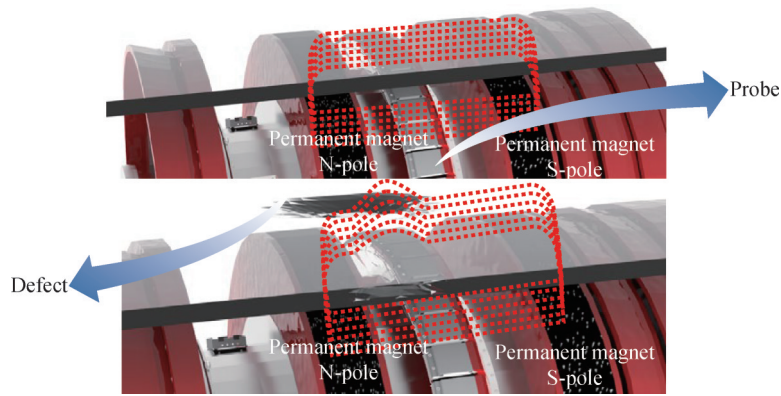


Fig.3 Basic Principle of Pipeline MFL ILI(Probe, S pole, Defect, Permanent magnet, S pole, N pole)

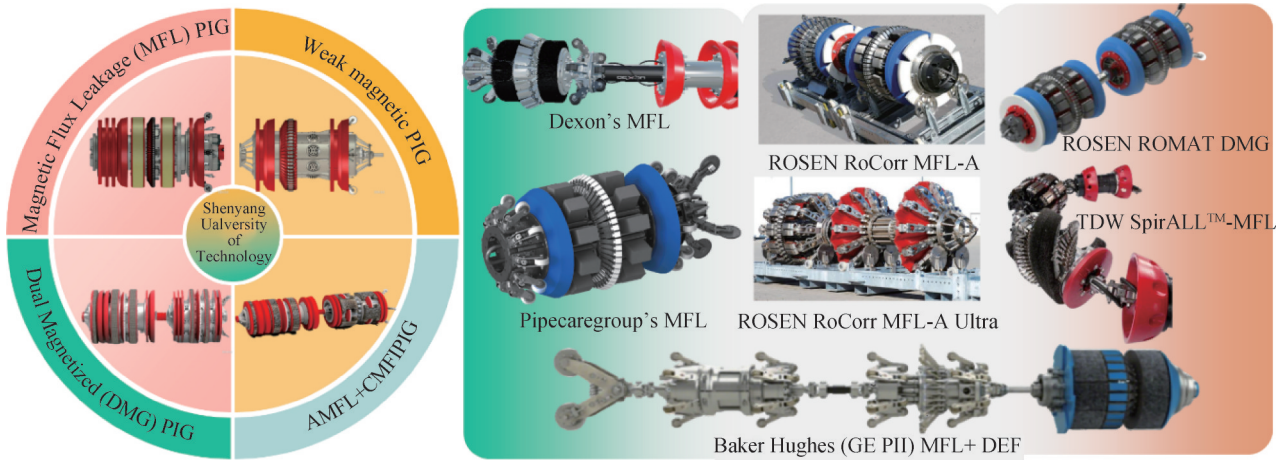


Fig.4 Mainstream Magnetic PIGs(Weak magnetic PIG, Dexon's MFL, ROSEN ROMAT DMG, ROSEN RoCorr MFL-A, Shenyang University of Technology, Dual Magnetic Field PIG, AMFL-CMF I PIG, Pipecaregroup's MFL, Baker Hughes (GE PII) MFL+ DEF)

inertial navigation), which work together to realize pipeline defect detection. The following is a simplified explanation according to structural function classification: Cup (drive + support): Drives the PIG to move axially along the pipeline through the pressure difference between the front and rear generated by the flow of oil and gas media in the pipeline; at the same time, it plays a radial support and centering role, avoiding direct contact between core components such as equipment probes and the pipe wall, and ensuring detection stability. Permanent magnet and steel brush (unique to MFL/DMG detectors): The combination of permanent magnet and steel brush constructs an axial magnetization field; the steel brush assists in optimizing the uniformity of the magnetic field and enhancing the recognizability of defect MFL signals. Speed regulation unit: Adjusts the pressure difference between the front and rear of the PIG by controlling the medium bypass flow, realizes the stable control of the traveling speed, and is a key auxiliary module to ensure detection consistency. Data processing unit: Real-time collects and temporarily stores magnetic signals, mileage data, and navigation data, providing original information correlation for subsequent defect identification and stress evaluation. Mileage wheel: Rotates synchronously with the PIG, measures the operating mileage through friction

with the inner pipe wall, correlates magnetic signal abnormalities with the physical position of the pipeline, and is the basic coordinate source for defect positioning. Inertial navigation: Relies on inertial sensors such as gyroscopes and accelerometers, does not depend on GPS signals, and only infers the real-time position and trajectory through the equipment's own motion state; corrects cumulative errors by combining with mileage wheel data to improve defect positioning accuracy. Connecting rod device: Through mechanical connection, it can connect PIG and pig in series to realize the coordination of multiple functions. Probe: Multiple magnetic sensors are usually installed on the PIG, distributed 360 degrees along the pipeline circumference, coated with wear-resistant ceramics and supported by flexible brackets, which can collect the magnetic signal fluctuations of the pipeline in all directions. The following sorts out the key parameters of several mainstream magnetic sensors to provide references for technical selection and application:

Table 3 lists the core performances of several commonly used magnetic field detection sensors: in terms of sensitivity, TMR > GMR > AMR > Hall; in terms of size, GMR > Hall ≈ AMR > TMR; in terms of resolution, TMR ≈ AMR > GMR > Hall; in terms of detection range, Hall > TMR > GMR > AMR. Due to

Table 3 Parameter Comparison of Magnetic Sensors for PIG

Sensor Type	Power Consumption (mA)	Size (mm)	Sensitivity (mV)	Detection Range(Gs)	Resolution (mGs)	
Hall sensor(Hall)	5~20	1×1	0.05	0.01~1000	500	
Magnetoresistive sensor	Anisotropic Magnetoresistive(AMR)	1 ~ 10	1×1	1	0.001 ~ 10	0.1
	Giant Magnetoresistive(GMR)	1 ~ 10	2×2	3	0.1 ~ 30	2
	Tunnel Magnetoresistive(TMR)	<0.01	0.5×0.5	20	0.001 ~ 200	0.1
Fluxgate sensor	10~50	3×3	10	0.001~1000	0.01	

different principles, these sensors have their own advantages: Hall sensors have a large detection range but low resolution, suitable for basic detection scenarios; magnetoresistive sensors have continuous breakthroughs in sensitivity and integration, but a small detection range, making them the first choice for micro-damage ILI.

### 3.1 Research Status of MFL-PIG

As the most mainstream ILI method, MFL is mainly aimed at volume defects such as metal loss, pitting corrosion, pinholes, and grooves. The main parameters of current international mainstream pipeline MFL-PIGs are compared as shown in Table 4.

As can be seen from Table 4, international energy industry inspection giants such as Rosen of Germany, Baker Hughes of the United States, and TDW of Russia are continuously promoting technological iteration and breakthroughs. Domestically, after more than 30 years of technological research, institutions such as CNPC Inspection (formerly Pipeline Technology Company of China National Petroleum Pipeline Bureau), National Pipeline Network Group, China Special Equipment Inspection and Research Institute, and Shenyang University of Technology have carried out in-depth research and accumulated solid results in the field of pipeline magnetic flux leakage internal detection, and their technical level has reached the US NACE ultra-high definition standard.

### 3.2 Development Trends of MFL ILI Technology

#### 3.2.1 Development Trends of MFL Forward Models

In forward research, the core is to construct an accurate MFL analytical model to clarify the mapping relationship between defect characteristics and magnetic signals, providing a theoretical basis for defect quantification. Edwards C. et al. established a one-dimensional magnetic leakage field mathematical model for surface-breaking cracks based on the ellipsoidal cavity theory and verified the feasibility of its extension to three-dimensional models, laying a foundation for the magnetic field analysis of complex-shaped defects<sup>[43]</sup>; Dutta S. et al. constructed a three-dimensional magnetic field calculation model based on Maxwell's equations,

describing the spatial characteristics of the three orthogonal components of the magnetic field varying with defect radius, depth, and magnetization intensity through the concept of dual magnetic charge conductors, deepening the understanding of the distribution law of leakage magnetic fields<sup>[44]</sup>; Suresh V. et al. proposed a first-type elliptic integral analytical model based on the magnetic dipole model, which can effectively predict the MFL signals of surface defects in ferromagnetic materials, improving the engineering applicability of the model<sup>[45]</sup>; Hosseingholizadeh S. et al. solved the MFL signals by combining the magnetic dipole model by determining the contour and size of the surface and volume magnetic charge densities near the defects, and verified the accuracy of the method with reference to numerical models, further improving the magnetic charge distribution theory<sup>[46]</sup>. Domestic scholars have also made significant progress in forward model optimization, especially focusing on the impact of non-uniform magnetic charge distribution on MFL signals: Zhong W. et al. first discovered the non-uniformity of magnetic charge distribution, providing an important basis for the correction factor of non-uniform magnetic charge distribution<sup>[47, 48]</sup>; Jin S. et al. proposed an equivalent magnetic charge method specifically for calculating the distribution of magnetic charge density on the pipeline surface<sup>[49]</sup>; Wu D. et al. analyzed the distribution of defect leakage magnetic fields through vector synthesis method, established a leakage magnetic field distribution model when the magnetization direction and defects are at any angle, and described the influence law of defect directionality on the distribution of leakage magnetic fields<sup>[50]</sup>; Wang Y. et al. proposed an improved magnetic dipole model, incorporating the influence of stress around cylindrical through-hole defects on MFL signals, expanding the application scenarios of the model in inverting defect shape and size<sup>[51]</sup>; Li G. et al. established a model of the influence of axial sampling interval on the magnetic flux leakage signals of pipeline circumferential cracks, and found that the increase of sampling interval leads to a precise logarithmic attenuation law of signal-to-noise ratio<sup>[52]</sup>; Li H. et al. proposed a magnetic charge element method based on magnetization microscopic mechanism and magnetic dipole model, which can quickly and accurately calculate the leakage magnetic field distribution of arbitrary defects<sup>[53]</sup>; Dong S. et al.

Table 4 Main Parameter Comparison of Mainstream Pipeline MFL-PIGs

Manufacturer/ Institution	Representative Product	Minimum Detection Depth (POD= 90%)	Depth Quantitative Accuracy (Confidence= 80%)	Length Quantitative Accuracy (Confidence =80%)	Width Quantitative Accuracy (Confidence e=80%)	Axial Positioning Accuracy	Circumfer- ential Positioning Accuracy	Applicable Pipe Diameter	Detection Object	Magnetization Method	Detectio n Speed
NACE [20]	NACE 35100 (Traditional)	10%t	±10%t	±20mm	±10mm	±0.1m (weld)	±5.0°	Full diameter compatible	Metal loss	Axial magnetization	0.5-5m/s
	NACE 35100 (Omnidirectional)	15%t -20%t	±15%t -20%t	±15-20mm	±15-20mm	±0.1m (weld)	±5.0°	Full diameter compatible	Metal loss + omnidirectio nal defects	Axial + circumferential dual magnetization	≤4m/s
Rosen [35]	RoCorr MFL-A	10%t	10%t	±15mm	±15mm	±0.1%l	±5.0°	Φ76.1mm-Φ 1400mm	Metal loss	Axial magnetization	≤3m/s
	RoCorr MFL-A Ultra	10%t	±0.4mm	±7mm	±8mm	±0.1%l	±10°	Φ76.1mm-Φ 1400mm	Metal loss	Axial magnetization	≤2.5m/s
	RoCorr MFL-C	10%t	10%t	±15mm	±15mm	±0.1%l	±5.0°	Φ152mm-Φ 1422mm	Metal loss + weld defects	Axial + circumferential dual magnetization	≤5m/s
Baker Hughes (PII) [36]	MagneScan™	Not marked	Not marked	Not marked	Not marked	Not marked	Not marked	Not marked	Metal loss + hard spots	Not marked	Not marked
TDW [37, 38]	SpirALL™-MFL	Not marked	Not marked	Not marked	Not marked	Not marked	Not marked	168.3-762mm	Metal loss + omnidirectio nal defects	Spiral magnetization	≤2.5m/s
Dexon [39]	Dexon's MFL	Not marked	±15%t	±18mm	±18mm	0.25%l	±10°	114.3-not marked mm	Metal loss	Axial magnetization	0.1-5 m/s
Pipecare [40]	Pipecaregroup's MFL	10%t	±10%t	±10mm	±15mm	0.2%l	±10°	60.3-1422mm	Metal loss	Axial magnetization	0.2 – 5m/s
Shenyang University of Technology [41]	Pipeline MFL-PIG	5%t	±10%t (Confidence= 90%)	±10mm	±10mm	±0.1%l	±5.0°	168.3- 1422mm	Metal loss	Axial magnetization	≤5m/s
	Omnidirectional Ultra- HD MFL-PIG	5%t	±10%t (Confidence= 90%)	±10mm	±10mm	±0.1%l	±5.0°	273-1219mm	Metal loss + omnidirectio nal defects	Axial + circumferential dual magnetization	≤5m/s
CNPC Inspection [42]	Pipeline Ultra-HD MFL Composite Detector	Not marked	Not marked	Not marked	Not marked	Not marked	Not marked	114.3- 1422mm	Metal loss	Axial magnetization	≤9m/s
	Transverse Excitation Detector	Not marked	Not marked	Not marked	Not marked	Not marked	Not marked	114.3- 1422mm	Metal loss + weld defects	Circumferential magnetization	≤9m/s

Note: t = pipe wall thickness; POD = Probability of Detection; l = calibration point spacing

proposed an ultra-high definition submillimeter-level pipeline MFL internal detection technology, enhancing the detection capability of weld defects, crack-like defects, and pinhole small defects<sup>[54]</sup>.

### 3.2.2 Development Trends of MFL Forward Models

Inversion research focuses on inverting key defect parameters from measured MFL signals through signal analysis and algorithm optimization to realize quantitative defect characterization. Zhang H. et al. proposed a defect size quantification method for pipeline magnetic flux leakage detection systems based on multi-level knowledge-guided neural networks, which effectively integrates prior knowledge and specific data<sup>[55]</sup>; Feng J. et al. adopted a pipeline MFL defect quantification method based on visual transformation, trained on 2800 mixed data (2000 simulated + 800 measured), and achieved a 7% wall thickness error in MFL defect depth quantification<sup>[56]</sup>; Liu J. et al. adopted a Multi-Level Knowledge-Guided Neural Network method, based on 383 training samples and 96 test samples of X65 pipelines, and pre-trained the network with simulated samples, resulting in a depth MAE of 0.216mm<sup>[57]</sup>; they also proposed an MFL defect quantification method under incomplete information based on icGANs, with a depth quantification error of less than 1mm<sup>[58]</sup>; subsequently, they proposed a network where the outputs of three CNNs supervise each other, tested with data from  $\Phi 325$  pipelines, and achieved an accuracy of 93.5%<sup>[59]</sup>; for irregular defects, they designed a pre-trained Vgg16 model and introduced feature parameters, trained with 280 irregular defects of varying shapes and sizes, and 35 for testing, indicating that the method can effectively quantify irregular defects<sup>[60]</sup>; Huang S. et al. proposed a right-angle feature opening profile recognition method fused with the z-axis component of magnetic signals, verifying the optimization effect of the z-axis component of magnetic signals on right-angle features based on finite element simulation data and experimental data<sup>[61]</sup>; proposed DfedResNet, introduced the magnetic dipole model into the loss function, used 243 artificial defects of X65 pipelines, expanded to 3321 data through depth interpolation for training and verification, with a depth quantification error  $\leq 0.4\%$ <sup>[62]</sup>; proposed a feature approximation method, approximated the signal features under zero lift-off through numerical fitting, accurately located the edges of arbitrary-shaped defects<sup>[63]</sup>, further improved the robustness of profile recognition, forming a technical progression from feature mining to intelligent quantification.

The refinement of forward models and the intelligence of inversion algorithms have jointly promoted the development of MFL technology towards higher precision, providing key technical support for the accurate quantitative detection of pipeline defects.

## 4 Oil and Gas Pipeline MFL ILI Technology

### 4.1 Research Status of LMFL-PIG Equipment

Traditional pipeline MFL has played a key role in the detection of macro volume defects such as corrosion, grooves, and metal loss, providing effective support for pipeline defect identification and accident prevention. However, this technology has significant limitations in identifying stress abnormalities: relying on "physical signals generated after defect formation", it cannot effectively evaluate stress concentration areas without formed volume defects (such as welding residual stress during construction, stress concentration due to foundation settlement, coupled stress between medium internal pressure and thermal expansion, etc.), making it difficult to early warn of sudden fracture and pipe burst accidents caused by stress accumulation.

To break through this technical bottleneck, pipeline LMFL ILI technology has emerged. Its theoretical origin can be traced back to the Metal Magnetic Memory (MMM) detection technology. Proposed by Russian scholar Professor Dubov at the 50th International Welding Conference in San Francisco, USA in 1997, this technology mainly utilizes the "magnetic memory effect" generated by ferromagnetic materials under the coupling action of stress and geomagnetic field (irreversible leakage magnetic field distortion will form in stress concentration areas) to realize the early identification of hidden stress damage<sup>[64]</sup>. However, early MMM mainly relied on external detection equipment, which had low automation and could not meet the ILI needs of long-distance pipelines.

In recent years, domestic and foreign research teams have continued to innovate on the basis of MMM technology: by optimizing magnetic sensitive sensors and developing long-endurance ILI carriers, they have successfully transformed the technology into LMFL-PIG. Without external strong excitation, relying on the coupling effect of geomagnetic field and pipeline stress field, it can operate continuously in pipelines and identify stress concentration areas. Some LMFL-PIGs have formed industry application specifications (Q/SY 05036-2018 Technical Specification for Weak Magnetic Stress Concentration Internal Detection of Oil and Gas Pipelines)<sup>[65]</sup>, filling the gap of traditional technologies in the field of "stress detection of unformed defects" and providing a new technical path for the whole-life cycle safety management of pipelines. The following systematically sorts out the technical progress of current pipeline LMFL-PIGs (including MMM external detection equipment) through performance index comparison:

### 4.2 Development Trends of LMFL ILI Technology

LMFL ILI technology is an emerging pipeline stress

Table 5 Main Parameter Comparison of Mainstream LMFL ILI (including MMM)

Manufacturer/ Institution	Representative Product	Detection Accuracy	Axial Positioning Accuracy	Circumferential Positioning Accuracy	Applicable Pipe Diameter	Detection Object	Magnetization Method	Detection Speed
TDW <sup>[66]</sup>	Low Field Magnetic Flux Leakage	Not marked	Not marked	Not marked	219.1 mm -762mm	Stress, hard spots, weld damage	Weak excitation mode	Not marked
Shenyang University of Technology	Weak Magnetic PIG	Magnetic field sensitivity 1nT	±0.1% l	±5.0°	273mm– 1219mm	Stress, weld damage	No external excitation	0.3–14.4m/s
Dynamic Diagnostics Company	TSC series MMM	Magnetic field sensitivity ≤ 5nT	External detection, not applicable	External detection, not applicable	External detection, not applicable	Stress, weld damage	No external excitation	0.2–0.5m/s (manual)
China Special Equipment Inspection and Research Institute <sup>[67]</sup>	Unsaturated magnetization (UNSM)	Experimental stage	Experimental stage	Experimental stage	Experimental stage	Experimental stage	Experimental stage	Experimental stage

ILI technology. Non-destructive stress detection technology has a long development history. Experts and teams at home and abroad have achieved good research results in the research of ray, ultrasonic, eddy current, Barkhausen<sup>[68]</sup> and other technologies, which can achieve stress detection to varying degrees. For example, Gao B. et al. designed a hybrid sensing structure for measuring eddy current, alternating field, Barkhausen noise, and incremental permeability signals to measure the stress of silicon steel sheets<sup>[69]</sup>; Liu X. et al. used magnetic Barkhausen technology and incremental permeability technology to measure the tensile stress of steel<sup>[70]</sup>, etc. These new technologies are important explorations in the stress detection of ferromagnetic materials, but due to their inability to meet the complex working conditions of pipeline internal inspection such as high speed, non-contact, and anti-interference, their application in the field of pipeline ILI is limited. LMFL ILI technology has good application potential in the field of pipeline stress ILI. Based on the magnetomechanical coupling effect of ferromagnetic materials, this technology realizes early damage assessment by measuring the spontaneous micro-magnetic signals caused by stress concentration areas or defects. Its core lies in establishing an accurate magnetomechanical constitutive relationship and signal forward model, which has been systematically studied by scholars at home and abroad.

Since Newton's laws and Maxwell's equations are difficult to establish the magnetomechanical coupling relationship, in the theoretical aspect of magnetomechanical properties, scholars at home and abroad have conducted research from different angles, developing micro-models based on atomic, lattice and other micro-scales to study the relationship between stress and magnetic moment, and macro-models based on continuum mechanics and other principles, helping the

engineering application of pipeline LMFL ILI technology.

#### 4.2.1 LMFL (MMM) Magnetomechanical Response Model Based on First-Principles

The magnetism of pipelines fundamentally originates from magnetic moments. First-principles calculation methods can calculate the corresponding relationships between parameters such as electron spin motion, electron orbital motion, and electron layout number and external force fields. By studying the corresponding relationship between magnetic signals and atomic magnetic moments, the MMM signal characteristics of stress damage areas of ferromagnetic components can be analyzed, and a non-contact, dynamic ILI mathematical model of magnetomechanics can be established. At present, there are many related studies at home and abroad. Yang L. et al. first proposed to explain the stress-magnetization relationship of materials based on first-principles, explained the basic principle of pipeline LMFL ILI, and verified that the atomic scale model can well predict the variation trend of MMM signals with stress through pipeline pressure test<sup>[71, 72]</sup>; Liu B. et al. further analyzed the magnetic moment changes of pipelines under different stress levels, conducted systematic experimental verification, proved the variation trend of MMM signals under different stresses<sup>[73-75]</sup>, explored the corresponding relationship between micro-scale metal properties and MMM signals<sup>[76, 77]</sup>, and proposed to use critical shear stress to characterize the critical damage state of pipelines, providing a further idea for atomic scale modeling [78]; Shi P. et al. explained the atomic scale mechanism of strain-induced magnetic changes in MMM, and calculated the effects of tensile stress, compressive stress, and doping on MMM signals<sup>[79]</sup>.

#### 4.2.2 LMFL Magnetomechanical Response Model Based on Constitutive Relationship

Compared with models based on first-principles, models based on constitutive relationships are easier to verify and optimize parameters through experiments, and model research is more extensive and close to actual conditions. Starting from 1984, Jiles D. and Atherton D. proposed the J-A model based on effective field theory and the approach principle of irreversible magnetization, which first quantified the nonlinear relationship between stress and magnetization, but the prediction accuracy was limited and it could not describe the influence of plastic deformation<sup>[80-83]</sup>. Subsequently, Sablik M. introduced a demagnetization term on the basis of the original model, established the relationship between saturation magnetostriction coefficient and stress based on Gaussian equation, modified the approach theorem in the J-A model<sup>[84-86]</sup>, and further extended the theory<sup>[87-90]</sup>.

Many scholars have conducted further research on the model. In terms of the improvement of the J-A magnetomechanical relationship, Liu Q. et al. modified the plastic deformation magnetization model<sup>[91]</sup>; Liu B. et al. studied the variation law of weak magnetic signals with stress direction, clarified the damage degree of stress in different directions to pipelines and the characteristics of MMM signals<sup>[92]</sup>, established a complex stress model suitable for pipelines<sup>[93]</sup>, established the transmission equation of MMM stress signals in different media, compensated for the attenuation of non-contact weak magnetic signals of pipeline MMM stress, and improved the theoretical model of non-contact online detection of pipeline MMM stress<sup>[94]</sup>; Zheng X. et al. established the Z-L model, introduced thermodynamic potential function, first quantitatively described the "flip phenomenon" of magnetostriction curve and stress  $\Delta E$  effect, and extended it to magneto-thermal-mechanical coupling scenarios<sup>[95]</sup>; Shi P. proposed an explicit ideal magnetization constitutive<sup>[96, 97]</sup>, modified the effective field expression caused by plastic deformation [98], derived the explicit analytical solution under the linear simplification of Langevin function, and the calculation efficiency was improved by 50%<sup>[99]</sup>; combined with the modification of approach principle and Rayleigh law, the contradiction of opposite signs in magnetization intensity prediction was solved. Luo X. et al. combined the nonlinear magnetostrictive strain relationship in the Z-L model and the hysteresis theory in the J-A model, considered the influence of stress and plastic deformation on model parameters, and established a modified magnetization model that can reflect the influence of elastic-plastic stress and strain on the magnetization curve of ferromagnetic materials<sup>[100]</sup>; Zhang L. et al. improved the magnetomechanical coupling relationship based on corrected magnetization and machine learning methods, which can effectively predict pipeline stress<sup>[101]</sup>.

In summary, the LMFL ILI magnetomechanical

response model based on constitutive relationship, from the pioneering quantification of the stress-magnetization relationship by the J-A model, to the modification of Sablik M. by introducing a demagnetization term, and then to the continuous optimization for scenarios such as plastic deformation, stress direction, and multi-field coupling, has gradually constructed a complete framework from basic theory to engineering application, providing core theoretical support for the breakthrough of LMFL ILI technology from qualitative positioning to quantitative evaluation.

## 5 Oil and Gas Pipeline DMG ILI Technology

DMG ILI technology integrates the advantages of MFL and LMFL. Through two sets of independent excitation systems (strong and weak), it utilizes the sensitivity difference of magnetic signals to stress under different excitation intensities to realize the accurate discrimination of pipeline defects and stress concentration areas and the quantitative analysis of composite defects. The structural frameworks of the two parts of DMG-PIG are consistent, and the core difference focuses on the excitation unit: the permanent magnet of the strong excitation detector has high magnetic field intensity, driving the pipeline wall to reach a magnetic saturation state, and the probe mainly collects the MFL signal of pure defects (directly characterizing the magnetic flux leakage distortion caused by the geometric characteristics of macro volume defects such as corrosion pits and metal loss); the permanent magnet of the weak excitation detector has low magnetic field intensity, maintaining the pipeline in a weak magnetization environment, and the signal detected by the probe includes the LMFL composite response of defects and stress<sup>[102]</sup>.

At present, regarding the research on DMG-PIG, Rosen of Germany has developed DMG detection equipment internationally, which can detect material hardness changes of  $\pm 50\text{HB}$  under 90% confidence [103]. The domestic equipment detection indicators can reach a magnetic field distribution rate of 5nT, a measurement range of  $\pm 5\text{mT}$ , and a detection confidence of stress concentration areas  $>95\%$ <sup>[104, 105]</sup>.

## 6 Oil and Gas Pipeline ECT ILI Technology

### 6.1 Research Status of ECT-PIG

ECT ILI technology generates eddy currents in conductive materials such as pipeline walls through alternating magnetic fields. Defects will interfere with the distribution of eddy currents, leading to changes in the impedance of the detection coil, thereby identifying surface or near-surface defects. The current mainstream ECT-PIGs are shown in Figure 5.

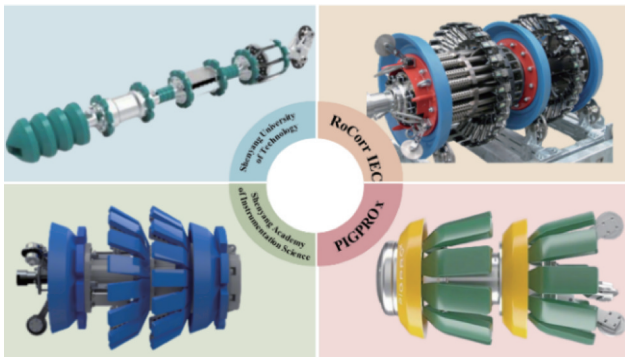


Fig.5 Mainstream ECT-PIGs(RoCorr IEC, Shenyang University of Technology, PIGPROX)

ECT ILI technology is a non-contact detection technology that does not require couplants and has high

sensitivity to surface defects. However, limited by the skin effect, the detection depth is usually less than 3-10mm, and it is greatly affected by the lift-off effect, resulting in low detection efficiency.

Table 6 shows the parameter comparison of current mainstream ECT-PIGs. It can be seen that Rosen's RoCorr IEC of Germany and domestic similar equipment have similar performances in terms of minimum detection depth, axial and circumferential positioning accuracy, etc., covering most common pipe diameters. There are differences in quantitative indicators of depth, length, width, and detection speed. The ECT-PIG developed by the University of Electronic Science and Technology of China-Sichuan Deyuan has the highest detection speed and can achieve high-precision defect quantification with 90% confidence.

Table 6 Main Parameter Comparison of Mainstream ECT-PIGs

Manufacturer/ Institution	Representative Product	Minimum Detection Depth (POD=90%)	Maximum Detection Depth	Depth Quantitative Accuracy (Confidence=80%)	Length Quantitative Accuracy (Confidence=80%)	Width Quantitative Accuracy (Confidence=80%)	Axial Positioning Accuracy	Circumferential Positioning Accuracy	Applicable Pipe Diameter	Detection Speed
Rosen <sup>[106]</sup>	RoCorr IEC	1.5mm	10mm	±1.3 mm	±6mm	±5mm	±0.1% l	±5.0°	168.3-1422mm	≤3m/s
i2 <sup>[107]</sup>	Pioneer	Not marked	Not marked	Not marked	Not marked	Not marked	Not marked	Not marked	≥88.9mm	0.1-7m/s
Shenyang Academy of Instrumentation Science <sup>[108]</sup>	Not marked	Not marked	Not marked	Not marked	Not marked	Not marked	Not marked	Not marked	Not marked	Not marked
University of Electronic Science and Technology of China-Sichuan Deyuan <sup>[109]</sup>	PIGPRO	1.5mm	10mm	±1.5mm (Confidence=90%)	±15mm (Confidence=90%)	±15mm (Confidence=90%)	±0.1% l	±5.0°	88.9-1219mm	0.1-8m/s
Shenyang University of Technology <sup>[110]</sup>	ECT-PIG	1.5mm	Not marked	±1.3mm	±6mm	±5mm	±0.1% l	±5.0°	273-1219mm	≤4m/s

Note: t = pipe wall thickness; POD = Probability of Detection; l = calibration point spacing

### 6.2 Development Trends of ECT ILI Technology

The current development trends of pipeline ECT ILI research mainly focus on sensor structure optimization, crack identification inversion, and detection system development: Hamia R. et al. proposed a new excitation method to improve deep crack detection capability<sup>[111]</sup>; Berkache A. et al. proposed horizontal eddy current to improve the signal-to-noise ratio of weld detection<sup>[112]</sup>; Repelianto A. S. et al. proposed a uniform eddy current probe to enhance the sensitivity to surface cracks of ferromagnetic materials<sup>[113]</sup>; Huang R. et al. optimized the eddy current calculation method, increasing the speed by 3 times<sup>[114]</sup>; Jin Z. et al. proposed a submillimeter-level

crack detection system to establish the corresponding relationship between signals and crack sizes<sup>[115]</sup>; Chen Z. et al. proposed a pipeline crack inversion method based on array eddy current probe signals<sup>[116]</sup>; Gao B. et al. proposed a multi-sensor signal defect analysis algorithm for pipeline electromagnetic internal detection based on Feature Boosting<sup>[117]</sup>, and developed an unbalanced sensing mode to alleviate the sensitivity decrease caused by resolution improvement<sup>[118, 119]</sup>; Chen J. et al. realized the detection of 0.2mm deep cracks through numerical simulation, and improved the quantitative signal recognition accuracy by means of the SSA-BP neural network<sup>[120]</sup>; He Y. et al. proposed a simplified analysis

model for eddy current detection, solving the problem of complex calculation or insufficient accuracy of traditional methods in asymmetric structure detection<sup>[121]</sup>. Currently, to break through the limitation of the traditional eddy current skin effect, pulsed eddy current testing (PECT)<sup>[122]</sup>, remote-field eddy current (RFEC)<sup>[123]</sup>, pulsed remote-field eddy current<sup>[124]</sup>, and alternating current field measurement (ACMF) have been derived. Yuan X. et al. detected surface and subsurface cracks based on the phase reversal characteristics of ACMF<sup>[125]</sup>; Tian G. et al. proposed a detection method combining PECT and RFEC to improve the probe resolution and penetration capability simultaneously<sup>[126]</sup>. The above indicates that ECT ILI technology is insensitive to crack direction, limited by the skin effect, and the lift-off effect will affect the amplitude and phase of detection signals. Solving these problems is the focus of current technical research.

## 7 Oil and Gas Pipeline BE ILI Technology

BE ILI technology adopts mutually forward excitation coils and detection coils. When there is no defect in the tested component, the electromagnetic balance state is maintained; when there is a defect in the tested component, the eddy current field and leakage magnetic field formed on the surface of the tested component by the orthogonal excitation coils and detection coils are used to detect surface and internal crack defects<sup>[127, 128]</sup>.

As an emerging electromagnetic non-destructive detection technology, BE ILI technology has few publicly available documents. It was first proposed by TesTex Company of the United States, and a crack offline detection system with a detection speed below 0.3m/s was developed, which can realize the detection of welds and surface and near-surface cracks within 3mm of the tested metal. The effectiveness of BE technology in detecting cracks in any direction on the pipeline surface, as well as the feasibility and applicability of ILI<sup>[129, 130]</sup>, a BE-PIG was developed to realize the detection of defects with a surface opening width greater than 0.1mm, and the detection accuracy of buried defects is  $\pm 3\text{mm}$ , which can effectively identify pipe body crack defects. Feng J. et al. proposed a multi-frequency BE technology, using a combination frequency of 400Hz and 20Hz to detect internal and external wall cracks of pipelines respectively, and studied the influence of the excitation frequency of multi-frequency balanced electromagnetic technology on crack angles and response signals of internal and external wall defects<sup>[131]</sup>. BE-PIG has good detection accuracy when the operating speed is less than 3m/s, and a speed control valve needs to be used to control the operating speed of the detector during engineering application.

## 8 Oil and Gas Pipeline PZT-UT ILI Technology

### 8.1 Research Status of PZT-UT-PIG

Pipeline piezoelectric PZT-UT ILI technology relies on piezoelectric elements to work. The transmitting end generates ultrasonic waves through inverse piezoelectric effect, and uses liquid couplants to reduce acoustic energy loss, enabling ultrasonic waves to efficiently propagate into the pipeline metal wall; when ultrasonic waves propagate in the pipe wall, they will be reflected when encountering defects such as corrosion and cracks. The receiving end converts the mechanical vibration of the reflected waves into electrical signals through piezoelectric effect, and realizes the positioning and quantitative analysis of defects after processing. PZT-UT transmits sound waves through inverse piezoelectric effect and receives sound waves through piezoelectric effect, requiring liquid couplants to ensure efficient acoustic energy transmission, so it is only suitable for oil transmission pipeline ILI. Figure 6 shows the mainstream PZT-UT-PIGs. The equipment mechanical structure is a multi-section series style, usually including energy drive section, detection section, electronic system section and other modules, with slightly different structural forms according to the requirements of applicable caliber, passing capacity, function combination, etc.

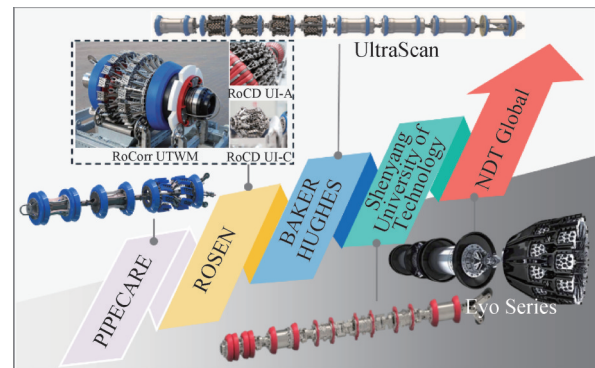


Fig.6 Mainstream PZT-UT PIGs (UltraScan, RoCD UTAI, NDT Global, Shenyang University of Technology, RoCD UT-CI, RoCorr UIWM, BAKER HUGHES, ROSEN, PIPECARE)

The performance indicators of mainstream international PZT-UT PIGs are listed below.

As can be seen from Table 7, the commercial application of PZT-UT PIG can be traced back to Baker Hughes of the United States, which developed the first set of pipeline axial crack PZT-UT PIG in 1994<sup>[139]</sup>. With the improvement of piezoelectric composite materials, sensors, electronics, and mechanical manufacturing technologies, the piezoelectric ultrasonic crack detection technology and equipment for oil and gas pipelines have made significant progress in detection accuracy, data processing, endurance, structural design, and passing performance. Many companies can provide PZT-UT ILI

Table 7 Main Parameter Comparison of Mainstream PZT-UT-PIGs

Manufacturer/ Institution	Equipment Name	Minimum Detection Depth (POD= 90%)	Depth Quantitative Accuracy (Confidence =80%)	Length Quantitative Accuracy (Confidence =80%)	Width Quantitative Accuracy (Confidence =80%)	Axial Positioning Accuracy	Circumferential Positioning Accuracy	Applicable Pipe Diameter	Applicable Object	Detection Speed
NACE [20]	NACE 35100	1mm	±0.4mm	±6mm	±12mm	±0.1m (weld)	±5°	Full diameter compatible	Defects	≤2m/s
Baker Hughes (PII) [26,132],	UltraScan™ CD/ CDP/CD Edge Series	Not marked	±0.7mm	±7.5mm	Not marked	±0.1m (weld)	±5°	Not marked	Not marked	Not marked
Rosen [133-135]	RoCorr UTWM	0.8mm	±0.4 mm	±7 mm	±8 mm	±0.1m (weld)	±10°	168.3- 1422mm	Corrosion	≤2.5m/s
	RoCD UT-A	1mm (pipe body) 2mm (weld)	±0.1 mm (< 4 mm)	±10 mm	Circumferen tial ±30 mm	±0.1m (weld)	±5°	114.3- 1422mm	Pipe body cracks, weld cracks, circumferential cracks	≤2m/s
	RoCD UT-C	1mm (pipe body) 2mm (weld)	±0.1 mm (< 4 mm)	±10 mm	Circumferen tial ±30 mm	±0.1m (weld)	±5°	168.3- 1422mm	Pipe body cracks, weld cracks, circumferential cracks	≤2m/s
NDT Global [136]	Evo Series 1.0 UC Type	1mm	±0.4mm	Not marked	Not marked	±0.1m (weld)	±10° (< 508mm); ±5° (≥ 508mm)	168.3- 1219mm	Corrosion	≤4m/s
PIPECARE [137]	UT INSPECTION TECHNOLOGY	1mm	±0.4mm	±5mm	±4mm	±0.2% l	±10°	60.3- 1422mm	Corrosion	0.2-2m/s
Shenyang University of Technology [138]	PZT-UT-PIG	0.8mm	±0.4 mm	±6mm	±12mm	±0.1m (weld)	±5°	88.9- 1219mm	Corrosion	≤2m/s
CNPC Inspection	UT Corrosion Detector	Not marked	Not marked	Not marked	Not marked	Not marked	Not marked	114.3- 1422mm	Corrosion	Not marked

t = pipe wall thickness; POD = Probability of Detection; l = calibration point spacing

services with similar performance.

## 8.2 Development Trends of PZT-UT ILI Technology

Oil and gas pipeline PZT-UT ILI technology has developed early, and currently, the detection mechanism and detection signal processing methods are relatively mature. The development trend of technical research focuses on sensor optimization and signal processing. In terms of piezoelectric sensors and coupling technology, the Institute of Mechanics, Chinese Academy of Sciences has developed flexible bendable sensors to realize non-destructive testing of curved surfaces<sup>[140]</sup>; Yang H. et al. proposed a spring-nut coupling device to solve the coupling problem of SH guided wave thickness measurement of high-temperature pipelines<sup>[141]</sup>; NDT Company realized high-temperature wall thickness detection through dry coupling waveguide strip technology<sup>[26]</sup>. In terms of signal processing and damage positioning, many studies have introduced nonlinear processing such as wavelet packet decomposition and kurtosis analysis to effectively suppress dynamic noise; in addition, Zeng Z. et al. proposed a probabilistic framework for damage characterization of tubular structures, which is used for ultrasonic guided wave detection and identification of early microcracks, providing a more rigorous theoretical support for the accurate positioning and quantitative evaluation of cracks<sup>[142]</sup>.

# 9 Oil and Gas Pipeline EMAT ILI Technology

## 9.1 Research Status of EMAT-PIG

Due to the limitation of PZT-UT ILI technology's dependence on couplants, the EMAT ILI system has gradually developed. Its technical principle is: using an electromagnetic coupling structure to excite and receive ultrasonic waves; the energized wire generates electromagnetic eddy currents on the surface of the tested workpiece; the eddy current particles vibrate under the action of electromagnetic mechanical force, thereby generating ultrasonic waves; the receiving coil of the EMAT transducer converts the received signals into electrical signals through the inverse mechanism of the excitation process, and realizes non-destructive testing through waveform processing and analysis.

Compared with traditional PZT-UT, EMAT does not require couplants and can directly perform detection on the surface of pipelines in high-temperature and high-pressure environments or with coatings, especially suitable for gas medium pipelines.

The performance indicators of relatively common international EMAT-PIGs are listed below.

As can be seen from Table 8, the high-resolution EMAT-PIG EmatScan CD developed by Baker Hughes of the United States and the RoCD EMAT series developed

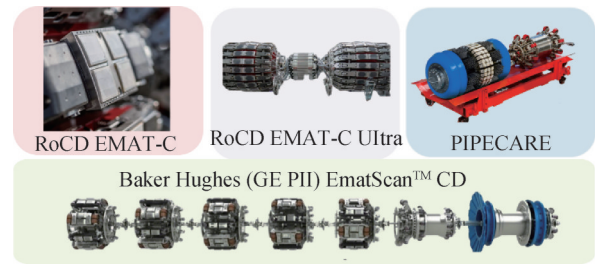


Fig.7 Mainstream EMAT-PIGs(RoCD EMAT-C, RoCD EMAT-C Ultra, PIPECARE, Baker Hughes (GE PII) EmatScan™ CD)

by Rosen of Germany can both realize pipeline crack and weld crack ILI. PIPECARE of the United States has also disclosed an EMAT-PIG, but the parameters are not specifically indicated.

## 9.2 Development Trends of EMAT ILI Technology

Currently, EMAT has achieved multi-dimensional breakthroughs in technical aspects such as transducer design, numerical simulation, and intelligent algorithms.

In terms of EMAT transducer structure optimization: Trushkevych O. et al. designed a new type of transducer that can detect millimeter-level defects, covering the range of length 1-11mm and depth 0.5-2mm<sup>[148]</sup>; Rieger K. et al. designed a magnet-free electromagnetic ultrasonic longitudinal wave transducer, the magnetic field on the surface of the tested piece reaches 3.2T when the coil lift-off is 2mm, and a pulse high-voltage independent module circuit is also designed<sup>[149]</sup>; Suresh N. et al. developed a variable magnet spacing EMAT, which evaluates the minimum residual thickness by using the cut-off characteristic of shear horizontal (SH) guided wave, and the maximum error of residual thickness measurement is 2.66%<sup>[150]</sup>; Takishita T. et al. developed a shear wave point-focusing EMAT transducer composed of a permanent magnet and two identical concentric meander coils, which can detect cracks 0.05mm deep on the bottom surface of 20mm thick stainless steel plates<sup>[151]</sup>; Thring C. et al. proposed a Rayleigh wave EMAT, fixing four coils under the magnet to increase the radiation angle of defect detection<sup>[152, 153]</sup>; Lee J. et al. proposed a single-coil and dual-coil omnidirectional lamb transducer in the plate to reduce signal interference<sup>[154, 155]</sup>; Huang S. et al. proposed a direction controllable EMAT based on magnetostrictive SH0 mode to increase the defect detection range<sup>[156]</sup>, and constructed physics-inspired deep neural networks (ProResNet, GuwNet), combining focused transducer design and guided wave quantification algorithms to achieve high-precision intelligent quantification of volume defects and crack defects, reducing dependence on large-scale datasets<sup>[157]</sup>; Kang Y. et al. designed a new type of dual AC magnetostrictive SH wave transducer based on the traditional static bias magnetostrictive SH wave theory, which improves the signal-to-noise ratio of signals<sup>[158]</sup>; Cen X. et al. optimized the transducer parameters and

Table 8 Main Parameter Comparison of Mainstream EMAT PIGs

Manufacturer/ Institution	Equipment Name	Minimum Detection Depth (POD=90%)	Depth Quantitative Accuracy (POD= 80%)	Length Quantitative Accuracy (POD=80%)	Axial Positioning Accuracy	Circumferential Positioning Accuracy	Applicable Pipe Diameter	Applicable Pipe Diameter	Applicable Object	Detection Speed
Baker Hughes (PII) [143]	EmatScan CD	Not marked	Not marked	Not marked	Not marked	Not marked	Not marked	Not marked	Pipe body cracks, weld cracks	Not marked
Rosen [144, 145]	RoCD EMAT-C	Pipe Body 1mm Weld 2mm	Not marked $t < 10\text{mm} \pm 0.15t$ $\geq 10\text{mm}$ $\pm 0.20t$	Not marked $\pm 20\text{ mm}$	Not marked Colonies (e.g. SCC colonies) $\pm 30\text{ mm}$	$\pm 0.1\text{m}$ (weld)	$\pm 10^\circ$	273- 1219mm	Pipe body cracks, weld cracks	$\leq 2.5\text{ m/s}$
	RoCD EMAT- C Ultra	Pipe Body 1mm 1mm (POD95%) Weld 2mm 3mm (POD90%) (POD95%)	$t < 10\text{mm} \pm 0.20t$ $\geq 10\text{mm}$ $\pm 0.25t$ (POD90%) $t < 10\text{mm} \pm 0.15t$ $\geq 10\text{mm}$ $\pm 0.20t$ (POD90%) $t < 10\text{mm} \pm 0.15t$ $\geq 10\text{mm}$ $\pm 0.20t$ (POD95%)	$\pm 20\text{ mm}$ (POD95%)	$\pm 30\text{ mm}$ (POD95%)	$\pm 0.1\text{m}$ (weld)	$\pm 10^\circ$	Not marked	Pipe body cracks, weld cracks	Not marked
PIPECARE [146]	EMAT inspection	Not marked	Not marked	Not marked	Not marked	Not marked	Not marked	Not marked	Not marked	Not marked
CNPC Inspection [147]	EMAT PIG	3mm (POD not marked)	Not marked	50mm (POD not marked)	Not marked	Not marked	Not marked	Not marked	Not marked	$\leq 2\text{ m/s}$

t = pipe wall thickness; POD = Probability of Detection; l = calibration point spacing

proved that the shear wave conversion efficiency of the butterfly coil is more ideal<sup>[159]</sup>; Guo Z. et al. designed an arch-shaped permanent magnet structure to excite S0 mode guided waves more efficiently<sup>[160]</sup>; Sun Z. et al. designed a three-channel EAMT transducer to detect pipeline thinning and make up for the lack of pipeline thickness data<sup>[161]</sup>; Tang Z. et al. designed a composite EMAT integrating thickness measurement and guided wave detection by superimposing spiral coils and folded coils, with an error of less than 0.1mm<sup>[162]</sup>; Zhai G. et al. realized multiple acquisition of echo signals at high temperatures below 450 degrees by superimposing double-layer coils in high-temperature EMAT<sup>[163]</sup>; He J. et al. designed a self-excited EMAT model of coils, which can generate Lamb waves without magnets<sup>[164]</sup>. In terms of EMAT signal processing research: Gao B. et al. derived the influence of lift-off on EAMT signals from mathematical models and proposed a new signal model for high lift-off EAMT<sup>[165]</sup>; Suñol F. et al. proposed a cross-correlation algorithm to determine the echo time difference without multiple measurements of reference waves, and the reference wave parameters can be adjusted in real time<sup>[166]</sup>; Yacef N. et al. combined Hilbert transform and matching pursuit to calculate the echo time interval through signal envelope<sup>[167]</sup>; Fang Z. et al. combined USO detection with multi-zero-crossing technology to solve the cycle skipping problem caused by waveform changes<sup>[168]</sup>; Jiao Y. et al. adopted EEMD and SSWT for signal preprocessing, combined with EM algorithm to fit echo parameters to improve accuracy<sup>[169]</sup>; Zhao S. et al. used VMD combined with wavelet threshold method to process high-temperature EMAT signals, with a calculation error of less than 2%<sup>[170]</sup>; Faysal A. et al. proposed a sensitive mode selection method, multiplying frequency domain energy entropy by time domain kurtosis to reduce white noise of intrinsic functions and maintain the optimal combination<sup>[171]</sup>. These technological breakthroughs not only improve the detection capability of EMAT under extreme working conditions but also solve problems such as weak signals and difficult defect quantification

## 10 Conclusion

This paper systematically compares the current mainstream ILI technologies, including magnetic methods, electromagnetic methods, and ultrasonic methods. Based on different detection principles, these technologies have their own focuses in terms of applicable materials, defect types, and scenarios: MFL excels in the detection of volume defects, LMFL focuses on early warning of stress damage, and DMG can quantify the stress concentration of composite defects; ECT is suitable for surface and near-surface cracks, while BE technology extends to the detection of buried microcracks; UT technology achieves the quantification of all types of defects with high precision, among which

EMAT is more adaptable to special environments such as high temperatures and no couplants. The characteristic differences of various technologies jointly construct a diversified detection system, providing clear technical selection references for pipeline safety operation and maintenance personnel.

In the future, pipeline ILI will develop in depth towards intelligence: by combining algorithms such as deep learning-based defect recognition and multi-source data fusion, the signal processing efficiency and defect quantitative accuracy will be improved; new composite detection technologies will be formed by integrating multi-physics coupling to break through the limitations of single technologies, realizing the automation of the detection process and the visualization of results. Aligning with Academician You Z's insights, advancing high-end sensor technology requires strengthening industry-education integration for talent cultivation, promoting collaborative innovation across stakeholders, and intensifying demonstration applications in national strategic projects. For pipeline ILI, this means prioritizing the independent R&D of high-end sensors—such as miniaturized, intelligent magnetic sensors and high-precision ultrasonic transducers—to address the "chokepoint" constraints of imported core components. By fostering a complete industrial ecosystem for sensor innovation, China can achieve technological autonomy in pipeline inspection, ensuring the security and resilience of its energy infrastructure.

At the same time, the accurate detection of composite defects with multiple types of defects coexisting, especially weld damage, remains a key challenge to be overcome. Due to the superposition of welding residual stress, heat-affected zones, and macro defects in the weld area, a complex damage mechanism is formed. Existing technologies are difficult to fully capture their coupling characteristics. Related detection mechanisms, sensor design, and algorithm optimization will become the core directions of future research to fill the current technical gaps.

### Author Contribution:

Bin Liu: Conceptualization; Validation; Funding acquisition. Zheng Lian: Writing – review and editing. Ye Tian: Conceptualization; Investigation. Xinyang Dong: Visualization; Methodology. Rongxue Li: Writing – original draft; Investigation. Liyao He: Validation; Formal analysis. Meng Li: Resources; Data curation. Lijian Yang: Supervision; Project administration.

### Acknowledgments:

The authors acknowledge Shenyang University of Technology, and United Pipeline Co., Ltd., Pipe Network Group (Xinjiang) for supporting this research work.

### Foundation Information:

This research was funded by Key Program of

National Natural Science Foundation of China (grant number. 62531017), General Program of National Natural Science Foundation of China (grant number. 62371315), General Program of National Natural Science Foundation of China (grant number. 62571348), Natural Science Foundation of Liaoning Province (grant number. 2025-MS-117), Key Program of the Department of Science and Technology of Liaoning Province (No. 2024JH2/102500072), Youth Science Fund Project of National Natural Science Foundation of China (grant number. 62301341), Applied Basic Research Program of the Department of Science and Technology of Liaoning Province (grant number. 2025JH2/101300013), Youth Program of the Department of Education of Liaoning Province (grant number. 200080762/070).

### Data Availability:

The authors declare that the main data supporting the findings of this study are available within the paper and its Supplementary Information files.

### Conflicts of Interest:

The authors declare no competing interests.

### Dates:

Received 15 January 2026; Accepted 25 March 2026; Published online 31 March 2026

## References

- [1] Pan M., He Y., Tian G., et al. (2012). Defect characterization using pulsed eddy current thermography under transmission mode and NDT applications [J]. *Ndt & E International* , 52, 28-36. DOI: 10.1016/j.ndteint.2012.08.007
- [2] Zhu H., Xu X., Song H., et al. (2018). Review of in-pipe inspection technology and system development in pipeline [J]. *Pipeline Technol. Equip.* , (3), 22-25. DOI: 10.3969/j.issn.1004-9614.2018.03.007
- [3] Li Q., Zhao M., Ren X., et al. (2019). Construction status and development trend of Chinese oil & gas pipeline [J]. *Oil-Gas Field Surf. Eng.* , 38 (S1), 14-17. DOI: 10.3969/j.issn.1006-6896.2019.z1.004
- [4] Li Q., Zhao M., Zhang B., et al. (2021). Current construction status and development trend of global oil and gas pipelines in 2020 [J]. *Oil & Gas Storage and Transportation* , 40 (12), 1330-1337+1348. DOI: 10.6047/j.issn.1000-8241.2021.12.002
- [5] Bahadori A. (2016). *Oil and gas pipelines and piping systems: Design, construction, management, and inspection* [M]. Gulf Professional Publishing.
- [6] China National Petroleum Corporation Economic and Technological Research Institute. (2025). *Energy Data Manual of China Petroleum Economic and Research Institute in 2025* [Z]. China National Petroleum Corporation Economic and Technological Research Institute.
- [7] Zhu C., Li X. (2022). Practice and thinking of operation mechanism reform for oil and gas pipeline network [J]. *Petroleum & Petrochemical Today* , 30 (08), 51-54. DOI: 10.3969/j.issn.1009-6809.2022.08.011
- [8] Gong J., Yin X., Li W., et al. (2022). Exploration on the function and operation mode of natural gas pipeline networks in energy internet [J]. *Oil & Gas Storage and Transportation* , 41 (06), 702-711. DOI: 10.6047/j.issn.1000-8241.2022.06.012
- [9] Liu M., Sun L. (2020). Thinking on future reform for China's provincial gas pipeline network [J]. *Petroleum & Petrochemical Today* , 28 (06), 1-9+34. DOI: 10.3969/j.issn.1009-6809.2020.06.001
- [10] Huang W., Li Y., Chen P. (2023). China's co2 pipeline development strategy under the strategy of carbon neutrality [J]. *Natural Gas Industry* , 43 (07), 1-9. DOI: 10.3787/j.issn.1000-0976.2023.07.001
- [11] Wang Y., Lyu Y., Yang W., et al. (2022). Review of research for accidents occurred in gas transportation pipeline in home and abroad [J]. *Process Equipment & Piping* , 59 (04), 78-84. DOI: 10.3969/j.issn.1009-3281.2022.04.015
- [12] Wang W., Zhao Y. (2025). Research on gas pipeline safety management measures based on analysis of typical accident incidents [J]. *Chemical Engineering Management* , (07), 108-110. DOI: 10.19900/j.cnki.ISSN1008-4800.2025.07.029
- [13] Wei M., Shi Y., Fan Z., et al. (2025). Mechanism of human factors in oil and gas pipeline accidents [J]. *Journal of Xi'an University of Science and Technology* , 45 (01), 108-116. DOI: 10.13800/j.cnki.xakjdxxb.2025.0110
- [14] Zhu T., Xie Y., Sun W., et al. (2025). Statistical analysis and countermeasure research on pressure pipeline accidents [J]. *Chemical Engineering & Equipment* , (01), 133-138. DOI: 10.3969/j.issn.1003-0735.2025.1.fjhg202501040
- [15] You Z., Zheng Y. (2024). Why it's important to focus on developing high-end sensor technology [J]. *Instrumentation* , 11(04), 1-3. DOI: 10.15878/j.instr.202400268
- [16] Posakony G. (1993). Integrity assurance of natural gas transmission pipelines [J]. *Applied Mechanics Reviews* . DOI: 10.1115/1.3120323
- [17] Standardization Administration of the People's Republic of China. (2023). *Steel pipelines - Requirements for geometric deformation, metal loss and other key detection items* [S]. GB/T 27699-2023.
- [18] National Energy Administration of the People's Republic of China. (2018). *Steel pipelines- Requirements for geometric deformation, metal loss and other key detection items* [S]. SY/T 6597-2018.
- [19] Pipeline Operators Forum. *Steel pipelines - Detection specifications for key items* [S]. POF 100.
- [20] NACE International. (2017). *In-line inspection (ILI) technology* [S]. NACE 35100-2017.
- [21] Yang L., Geng H., Gao S. (2016). Magnetic flux leakage internal detection technology of the long distance oil pipeline [J]. *Chinese Journal of Scientific Instrument* , 37(08), 1736-1746. DOI: 10.3969/j.issn.0254-3087.2016.08.005
- [22] Min X., Yang L., Wang G., et al. (2017). Weak magnetism stress internal testing technology of the long distance oil-gas

- pipeline [J]. *Journal of Mechanical Engineering* , 53(12), 19-27. DOI: 10.3901/JME.2017.12.019
- [23] Tian Y., Chen H., Gao F., et al. Pipeline stress detection based on dual-field stress-magnetic coupling [J/OL]. *Journal of Shenyang University of Technology* , 1-11. DOI: 10.7688/j.issn.1000-1646.2025.05.09
- [24] Xuan W., Wang T., Dai L., et al. (2021). Feasibility of eddy current inline inspection for crack-like defects of oil and gas pipelines [J]. *Oil & Gas Storage and Transportation* , 40(12), 1384-1389+1440. DOI: 10.6047/j.issn.1000-8241.2021.12.009
- [25] Yang L., Zheng W., Li J., et al. (2021). Full-angle detection method of pipeline crack based on balanced electromagnetic technology [J]. *Chinese Journal of Scientific Instrument* , 42(06), 103-112. DOI: 10.19650/j.cnki.cjsi.J2107735
- [26] Kong C., Li Z., Qiu C., et al. (2024). Progress of piezoelectric ultrasonic in-line inspection technology for pipeline crack [J]. *Nondestructive Testing* , 46(12), 44-50. DOI: 10.11973/wsjc240172
- [27] Wei Y., Han Z., Guo D. (2021). Research on online electromagnetic ultrasonic testing system for wall thickness of urban gas pipeline [J]. *Instrument Technique and Sensor* , (11), 73-77+120. DOI: 10.3969/j.issn.1002-1841.2021.11.015
- [28] Lu R., Wang B., Wang H., et al. (2024). Self-driven continuous scanning in-line inspection system for industrial pipeline wall thickness based on electromagnetic ultrasound [J]. *Instrument Technique and Sensor* , (7), 94-99+104. DOI: 10.3969/j.issn.1002-1841.2024.07.017
- [29] Grand View Research. (2024). Pipeline pigging services market (2024-2030): size, share & trends analysis report [R]. <https://www.grandviewresearch.com/industry-analysis/pipeline-pigging-services-market>.
- [30] Rosen Group. In-line inspection services for deformation, geometry and mapping [EB/OL]. <https://www.rosen-group.com/en/expertise/product-and-service-finder/in-line-inspection-services-for-deformation-geometry-and-mapping#ro-geo-md-service>.
- [31] Dexon Technology. Caliper pigging services & location mapping [EB/OL]. <https://dexon-technology.com/pipeline-services/intelligent-pigging/caliper-pigging>.
- [32] Pipecare Group. Geometry pig (caliper inspection) service [EB/OL]. <https://www.pipecaregroup.com/caliper-inspection/>.
- [33] Shenyang Lujie Pipeline Technology Co., Ltd. Pipeline geometry internal detector [EB/OL]. <https://www.syljgd.com/product/guan-dao-ji-he-nei-jian-ce-qi/>.
- [34] National Natural Science Foundation of China. (2001). Scientists develop a high-precision intelligent online magnetic flux leakage detection system for pipelines, breaking foreign technological blockade and possessing independent intellectual property rights [R]. Briefing, (20), 1-4.
- [35] Rosen Group. In-line inspection services for corrosion [EB/OL]. <https://www.rosen-group.com/en/expertise/product-and-service-finder/in-line-inspection-services-for-corrosion#ro-corr-mfl-a-ultra-service>.
- [36] Baker Hughes. In-line inspection [EB/OL]. <https://www.bakerhughes.com/cn/node/128206>.
- [37] T. D. Williamson. Spirall® magnetic flux leakage (SMFL) [EB/OL]. <https://www.tdwilliamson.com/solutions/pipeline-integrity/inline-inspection/smfl>.
- [38] Pgonline. T. D. Williamson introduces spiral magnetic flux leakage inspection tool [EB/OL]. <https://pgionline.com/magazine/2011/february-2011-vol-238-no-2/technotes/td-williamson-introduces-spiral-magnetic-flux-leakage-inspection-tool>.
- [39] Dexon Technology. Magnetic flux leakage (MFL) in-line inspection services [EB/OL]. <https://dexon-technology.com/pipeline-services/intelligent-pigging/mfl-pigging>.
- [40] Pipecare Group. Magnetic flux leakage testing. MFL pipeline inspection [EB/OL]. <https://www.pipecaregroup.com/mfl-inspection/>.
- [41] Shenyang Lujie Pipeline Technology Co., Ltd. Ultra-high definition all-directional magnetic flux leakage internal detector [EB/OL]. <https://www.syljgd.com/product/guan-dao-chao-gao-qing-quan-fang-wei-lou-ci-nei-jian-ce-qi/>.
- [42] Li Z., Chang L., Zhang X., et al. (2023). Development of ultra-high definition magnetic flux leakage composite pipeline detector for  $\Phi 1016$  mm pipelines [J]. *China Petroleum Machinery* , 51(07), 138-145. DOI: 10.16082/j.cnki.issn.1001-4578.2023.07.018
- [43] Edwards C., Palmer S. (1986). The magnetic leakage field of surface-breaking cracks [J]. *Journal of Physics D: Applied Physics* , 19(4), 657. DOI: 10.1088/0022-3727/19/4/018
- [44] Dutta S., Ghorbel F., Stanley R. (2009). Dipole modeling of magnetic flux leakage [J]. *IEEE Transactions on Magnetics* , 45(4), 1959-1965. DOI: 10.1109/TMAG.2008.2011895
- [45] Suresh V., Abudhahir A. (2016). An analytical model for prediction of magnetic flux leakage from surface defects in ferromagnetic tubes [J]. *Measurement Science Review* , 16(1), 8. DOI: 10.1515/msr-2016-0002
- [46] Hosseingholizadeh S., Filleter T., Sinclair A. (2019). Evaluation of a magnetic dipole model in a dc magnetic flux leakage system [J]. *IEEE Transactions on Magnetics* , 55(4), 1-7. DOI: 10.1109/TMAG.2019.2897669
- [47] Zhong W. (2002). The linear magnetic charge density along the edges of a longitudinally-magnetized steel cuboid [J]. *Nondestructive Testing* , 24(8), 332-335. DOI: 10.3969/j.issn.1000-6656.2002.08.003
- [48] Zhong W. (1997). Theoretical fundamental of magnetic dipole for longitudinal magnetization of a square steel [J]. *Nondestructive Testing* , 19(4), 95-98.
- [49] Huang X., Chen S., Guo S., Zhao W., Jin S. (2013). Magnetic charge and magnetic field distributions in ferromagnetic pipe [J]. *Applied Computational Electromagnetics Society Journal* , 28(8): 737-746.
- [50] Wu D., Liu Z., Wang X., et al. (2017). Mechanism analysis of influence of surface-breaking orientation on magnetic leakage field distribution [J]. *Acta Physica Sinica* , 66(004), 293-304. DOI: 10.7498/aps.66.048102
- [51] Wang Y., Liu X., Wu B., et al. (2018). Dipole modeling of

- stress-dependent magnetic flux leakage [J]. *Ndt & E International* , 95, 1-8. DOI: 10.1016/j.ndteint.2018.01.004
- [52] Li G., Liu B., Zhou Y. (2025). Study on the influence of axial sampling spacing on MFL signals from circumferential cracks in pipelines [J]. *Oil & Gas Storage and Transportation* , 44 (10), 1149-1156. DOI: 10.6047/j.issn.1000-8241.2025.10.007
- [53] Zhang S., Li H., Zhao C. (2022). Magnetic-charge element method for magnetic flux leakage inspection [J]. *IEEE Transactions on Instrumentation and Measurement* , 71, 1-10. DOI: 10.1109/TIM.2022.3220273
- [54] Dong S., Tian Z., Lai S., et al. (2022). Research and application of a new generation of ultra-high-definition inline detection technology with sub-millimeter precision [J]. *Oil & Gas Storage and Transportation* , 41(01), 34-41. DOI: 10.6047/j.issn.1000-8241.2022.01.005
- [55] Wang L., Zhang H., Liu J., et al. (2022). Defect size quantification for pipeline magnetic flux leakage detection system via multilevel knowledge-guided neural network [J]. *IEEE Transactions on Industrial Electronics* , 70(09), 9550-9560. DOI: 10.1109/TIE.2022.3210557
- [56] Lu S., Feng J., Zhang H., et al. (2018). An estimation method of defect size from MFL image using visual transformation convolutional neural network [J]. *IEEE Transactions on Industrial Informatics* , 15(01), 213-224. DOI: 10.1109/TII.2018.2828811
- [57] Wang L., Zhang H., Liu J., et al. (2022). Defect size quantification for pipeline magnetic flux leakage detection system via multilevel knowledge-guided neural network [J]. *IEEE Transactions on Industrial Electronics* , 70(09), 9550-9560. DOI: 10.1109/TIE.2022.3210557
- [58] Fu M., Liu J., Zhang H., et al. (2020). Multisensor fusion for magnetic flux leakage defect characterization under information incompleteness [J]. *IEEE Transactions on Industrial Electronics* , 68(05), 4382-4392. DOI: 10.1109/TIE.2020.2984444
- [59] Jiang L., Zhang H., Liu J., et al. (2022). A multisensor cycle-supervised convolutional neural network for anomaly detection on magnetic flux leakage signals [J]. *IEEE Transactions on Industrial Informatics* , 18(11), 7619-7627. DOI: 10.1109/TII.2022.3146152
- [60] Jiang L., Zhang H., Liu J., et al. (2023). Pipeline irregular defect inversion for magnetic flux leakage detection system based on heterogeneous multiclass feature fusion [J]. *IEEE Transactions on Instrumentation and Measurement* , 72, 1-9. DOI: 10.1109/TIM.2023.3265110
- [61] Huang S., Peng L., Wang Q., et al. (2018). An opening profile recognition method for magnetic flux leakage signals of defect [J]. *IEEE Transactions on Instrumentation and Measurement* , 68(06), 2229-2236. DOI: 10.1109/TIM.2018.2869438
- [62] Sun H., Peng L., Huang S., et al. (2021). Development of a physics-informed doubly fed cross-residual deep neural network for high-precision magnetic flux leakage defect size estimation [J]. *IEEE Transactions on Industrial Informatics* , 18(03), 1629-1640. DOI: 10.1109/TII.2021.3089333
- [63] Long Y., Huang S., Peng L., et al. (2021). A characteristic approximation approach to defect opening profile recognition in magnetic flux leakage detection [J]. *IEEE Transactions on Instrumentation and Measurement* , 70, 1-12. DOI: 10.1109/TIM.2021.3050185
- [64] Dubov A. (1997). A study of metal properties using the method of magnetic memory [J]. *Metal Science & Heat Treatment* , 39(9), 401-405. DOI: 10.1007/BF02469065
- [65] China National Petroleum Corporation. (2018). Technical specification for weak magnetic stress concentration internal detection of oil and gas pipelines [S]. Q/SY 05036-2018.
- [66] T.D. Williamson. Low field magnetic flux leakage (LFM)[EB/OL]. <https://www.tdwilliamson.com/solutions/pipeline-integrity/inline-inspection/lfm>.
- [67] Xin J., Chen J., He R., et al. (2024). A novel stress concentration inspection method for marine oil and gas pipeline based on UNSM [J]. *Ocean Engineering* , 300, 117497. DOI: 10.2139/ssrn.4670641
- [68] Zhang Z., Shi P., Gou X. (2022). Analytical model of magnetic barkhausen stress test offerromagnetic plates [J]. *Acta Physica Sinica* , 71(09), 308-316. DOI: 10.7498/aps.71.20212253
- [69] Liu Y., Liu Q., Gao R., Gao B., Tian G. (2023). Stress measurement of ferromagnetic materials using hybrid magnetic sensing [J]. *IEEE Transactions on Instrumentation and Measurement* , 72, 1-13. DOI: 10.1109/TIM.2023.3280490
- [70] Wang N., Li P., Li T., Wang Y., He C., Liu X. (2024). Quantitative characterization of tensile stress in electroplated nickel coatings with a magnetic incremental permeability sensor [J]. *Sensors and Actuators A: Physical* , 368, 115082. DOI: 10.1016/j.sna.2024.115082
- [71] Yang L., Liu B., Gao S., et al. (2013). First principles calculation and experimental study of metal magnetic memory effects [J]. *Acta Physica Sinica* , 62(08), 399-405. DOI: 10.7498/aps.62.086201
- [72] Yang L., Liu B., Gao S., et al. (2013). Mechanism study on magnetic memory signal based on density functional theory [J]. *Chinese Journal of Scientific Instrument* , 34(04), 809-816. DOI: 10.3969/j.issn.0254-3087.2013.04.015
- [73] Liu B., Cao Y., Fu Y., et al. (2015). Study on magnetic memory signal characteristics based on NCPP plane wave algorithm [J]. *Chinese Journal of Scientific Instrument* , 36 (07), 1538-1545. DOI: 10.3969/j.issn.0254-3087.2015.07.012
- [74] Liu B., Cao Y., Wang G. (2016). Study on the characteristics of magnetic memory signal of phase transition point based on the LAPW algorithm [J]. *Chinese Journal of Scientific Instrument* , 37(08), 1825-1832. DOI: 10.3969/j.issn.0254-3087.2016.08.014
- [75] Liu B., Cao Y., Wang D., et al. (2017). Quantitative analysis of the magnetic memory yielding signal characteristics based on the LMTO algorithm [J]. *Chinese Journal of Scientific Instrument* , 38(06), 1413-1420. DOI: 10.3969/j.issn.0254-

- 3087.2017.06.012
- [76] Liu B., He L., Rao X., et al. (2017). Magnetic electronic exchange model and performance of quantitative analysis of the magnetic memory signals [J]. *Chinese Journal of Scientific Instrument*, 38(11), 2744-2751. DOI: 10.3969/j.issn.0254-3087.2017.11.016
- [77] Liu B., He L., Huo X., et al. (2017). Study on the mmm signal characteristics in magnetic field based on KP perturbation algorithm [J]. *Chinese Journal of Scientific Instrument*, 38(01), 151-158. DOI: 10.3969/j.issn.0254-3087.2017.01.020
- [78] Liu B., Tian R., Yu H., et al. (2024). Research on the characteristics of weak magnetic internal detection signals for critical damage in pipeline stress based on density functional theory [J]. *Engineering Failure Analysis*, 159, 108145. DOI: 10.1016/j.engfailanal.2024.108145
- [79] Wang S., Liang T., Shi P. (2022). Mechanism of strain-induced magnetic properties changes for metal magnetic memory technology on atomic scale [J]. *Acta Physica Sinica*, 71(19), 305-315. DOI: 10.7498/aps.71.20220745
- [80] Jiles D., Atherton D. L. (1984). Theory of ferromagnetic hysteresis [J]. *Journal of Applied Physics*, 55(6), 2115-2120. DOI: 10.1063/1.333582
- [81] Jiles D., Atherton D. L. (1986). Theory of ferromagnetic hysteresis [J]. *Journal of Magnetism and Magnetic Materials*, 61(1-2), 48-60. DOI: 10.1016/0304-8853(86)90066-1
- [82] Sablik M., Jiles D. C. (1988). A model for hysteresis in magnetostriction [J]. *Journal of Applied Physics*, 64(10), 5402-5404. DOI: 10.1063/1.342383
- [83] Ramesh A., Jiles D., Roderick J. (1996). A model of anisotropic anhysteretic magnetization [J]. *IEEE Transactions on Magnetics*, 32(5), 4234-4236. DOI: 10.1109/20.539344
- [84] Sablik M. J. (1997). A model for asymmetry in magnetic property behavior under tensile and compressive stress in steel [J]. *IEEE Transactions on Magnetics*, 33(05), 3958 - 3960. DOI: 10.1109/20.619628
- [85] Li L., Jiles D. C. (2003). Modified law of approach for the magnetomechanical model: application of the rayleigh law to stress [J]. *IEEE Transactions on Magnetics*, 39(05), 3037-3039. DOI: 10.1109/TMAG.2003.815882
- [86] Sablik M. J., Chen Y., Jiles D. C. (2000). Modified law of approach for the magnetomechanical model [C]//AIP Conference Proceedings, 509(01), 1565-1565. DOI: 10.1063/1.1306220
- [87] Sablik M. J., Stegemann D., Krysa A. (2001). Modeling grain size and dislocation density effects on harmonics of the magnetic induction [J]. *Journal of Applied Physics*, 89(11), 7254-7256. DOI: 10.1063/1.1355342
- [88] Sablik M. J. (2001). Modeling the effect of grain size and dislocation density on hysteretic magnetic properties in steels [J]. *Journal of Applied Physics*, 89(10), 5610-5613. DOI: 10.1063/1.1359167
- [89] Lo C. C. H., Kinser E., Jiles D. C. (2003). Modeling the interrelating effects of plastic deformation and stress on magnetic properties of materials [J]. *Journal of Applied Physics*, 93(10), 6626-6628. DOI: 10.1063/1.1557356
- [90] Sablik M. J., Yonamine T., Landgraf F. J. G. (2004). Modeling plastic deformation effects in steel on hysteresis loops with the same maximum flux density [J]. *IEEE Transactions on Magnetics*, 40(05), 3219-3226. DOI: 10.1109/TMAG.2004.832763
- [91] Liu Q., Luo X., Zhu H., et al. (2017). Modeling plastic deformation effect on the hysteresis loops of ferromagnetic materials based on modified jiles-atherton model [J]. *Acta Physica Sinica*, 66(10), 297-306. DOI: 10.7498/aps.66.107501
- [92] Liu B., Sun J., He L., et al. (2023). Quantitative study on internal detection signal of weak magnetic stress in oil and gas pipelines based on force-magnetic noncoaxial effect [J]. *Measurement*, 215, 112870. DOI: 10.1016/j.measurement.2023.112870
- [93] Liu B., Zheng S., He L., et al. (2019). Study on internal detection in oil-gas pipelines based on complex stress magnetomechanical modeling [J]. *IEEE Transactions on Instrumentation and Measurement*, 69(07), 5027-5036. DOI: 10.1109/TIM.2019.2956363
- [94] Liu B., Ma Z., He L., et al. (2018). Quantitative study on the propagation characteristics of mmm signal for stress internal detection of long distance oil and gas pipeline [J]. *NDT & E International*, 100, 40-47. DOI: 10.1016/j.ndteint.2018.08.006
- [95] Jin K., Kou Y., Zheng X. (2012). A nonlinear magneto-thermo-elastic coupled hysteretic constitutive model for magnetostrictive alloys [J]. *Journal of Magnetism and Magnetic Materials*, 324(12), 1954-1961. DOI: 10.1016/j.jmmm.2012.01.028
- [96] Shi P., Jin K., Zheng X. (2016). A general nonlinear magnetomechanical model for ferromagnetic materials under a constant weak magnetic field [J]. *Journal of Applied Physics*, 119(14), 145-153. DOI: 10.1063/1.4945766
- [97] Shi P., Jin K., Zheng X. (2017). A magnetomechanical model for the magnetic memory method [J]. *International Journal of Mechanical Sciences*, 124, 229-241. DOI: 10.1016/j.ijmecsci.2017.03.001
- [98] Shi P., Bai P., Chen H., et al. (2020). The magneto-elastoplastic coupling effect on the magnetic flux leakage signal [J]. *Journal of Magnetism and Magnetic Materials*, 504, 166669. DOI: 10.1016/j.jmmm.2020.166669
- [99] Shi P. (2021). Theoretical model of magneto-elastoplastic coupling for micro magnetic non-destructive testing method with stress concentration and plastic zone [J]. *Chinese Journal of Theoretical and Applied Mechanics*, 53(12), 3341-3353. DOI: 10.6052/0459-1879-21-325
- [100] Luo X., Zhu H., Ding Y. (2019). A modified model of magneto-mechanical effect on magnetization in ferromagnetic materials [J]. *Acta Physica Sinica*, 68(18), 295-306. DOI: 10.7498/aps.68.20190765
- [101] Dang H., Zhang L., Fan J., et al. (2025). Research on pipeline stress detection technology based on corrective magnetization and machine learning [J]. *Journal of Safety Science and*

- Technology* , 21(04), 27-33. DOI: 10.11731/j.issn.1673-193x.2025.04.004
- [102]Lian Z., Liu B., Liu T., et al. (2023). Research on the stress signal extraction method of pipeline composite defect based on dual magnetic field [J]. *Chinese Journal of Scientific Instrument* , 44(03), 107-118. DOI: 10.19650/j.cnki.cjsi.J2209693
- [103]Rosen Group. In-line inspection services for material properties [EB/OL]. <https://www.rosen-group.com/en/expertise/product-and-service-finder/in-line-inspection-services-for-material-properties#ro-mat-dmg-service>.
- [104]Shenyang Lujie Pipeline Technology Co., Ltd. Pipeline dual-field stress internal detector [EB/OL]. <https://www.syljgd.com/product/guan-dao-shuang-chang-ying-li-nei-jian-ce-qi/>.
- [105]Liu B., Luo N., Wu Z., et al. (2024). Research on non-volume damage of pipeline based on dual magnetic field detection [J]. *Chinese Journal of Scientific Instrument* , 45(08), 77-91. DOI: 10.19650/j.cnki.cjsi.J2412812
- [106]Rosen Group. In-line inspection services for corrosion [EB/OL]. <https://www.rosen-group.com/en/expertise/product-and-service-finder/in-line-inspection-services-for-corrosion#ro-corr-iec-service>.
- [107]I2I Pipelines. Pipeline inspection products [EB/OL]. <https://www.i2ipipelines.com/products/>.
- [108]Shenyang Academy of Instrumentation Science Co., Ltd. Pipeline inspection equipment [EB/OL]. [https://www.hb-sais.com/product\\_detail/247.html](https://www.hb-sais.com/product_detail/247.html).
- [109]Pigprox. Eddy flex [EB/OL]. [https://www.pigprox.com/pigprox\\_product/show-1.html](https://www.pigprox.com/pigprox_product/show-1.html).
- [110]Shenyang Lujie Pipeline Technology Co., Ltd. Pipeline eddy current corrosion internal detection equipment [EB/OL]. <https://www.syljgd.com/pro-duct/guan-dao-wo-liu-fu-shi-nei-jian-ce-she-bei/>.
- [111]Hamia R., Cordier C., Dolabdjian C. (2014). Eddy-current non-destructive testing system for the determination of crack orientation [J]. *NDT & E International* , 61, 24-28. DOI: 10.1016/j.ndteint.2013.09.005
- [112]Berkache A., Lee J., Wang D., et al. (2022). Development of an eddy current test configuration for welded carbon steel pipes under the change in physical properties [J]. *Applied Sciences* , 12(1), 93. DOI: 10.3390/app12010093
- [113]Repelianto A. S., Kasai N. (2019). The improvement of flaw detection by the configuration of uniform eddy current probes [J]. *Sensors* , 19(2), 397. DOI: 10.3390/s19020397
- [114]Huang R., Lu M., Peyton A., et al. (2020). A novel perturbed matrix inversion based method for the acceleration of finite element analysis in crack-scanning eddy current NDT [J]. *IEEE Access* , 8, 12438-12444. DOI: 10.1109/ACCESS.2020.2966032
- [115]Jin Z., Abe M., Oogane M., et al. (2017). Estimation of surface crack dimensional characteristics by an eddy current method using a single magnetic tunnel junction device [J]. *Japanese Journal of Applied Physics* , 56(7), 073001. DOI: 10.7567/JJAP.56.073001
- [116]Guo W., Zhao Y., Yang M., et al. (2025). A numerical scheme for crack reconstruction in tubes by signals of array eddy current testing probe [J]. *Acta Mechanica Solida Sinica* , 1-9. DOI: 10.1007/s10338-025-00604-w
- [117]Fu Y., Zhang Y., Mao Y., et al. (2024). Feature boosting framework for pipeline multi-sensing defects inspection using an intelligent pig system [J]. *Journal of Mechanical Engineering* , 60(20), 51-67. DOI: 10.3901/JME.2024.20.051
- [118]Zhou J., Ma Q., Gao B., et al. (2025). High-resolution pipeline in-line inspection based on non-equilibrium sensing with uneven electromagnetic distribution [J]. *NDT & E International* , 155, 103415. DOI: 10.2139/ssrn.5138300
- [119]Gao B., Tang Q., Ma Q., et al. (2025). Electromagnetic multi-physics quasi-uniform field layered-focusing sensing technology and its application in pipeline in-line inspection [J]. *China Measurement & Test* , 51(9), 113-128. DOI: 10.11857/j.issn.1674-5124.2025070075
- [120]Wang C., Chen J., Xin J., et al. (2022). Eddy current identification of pipeline cracks based on ssa-bp neural network [J]. *China Petroleum Machinery* , 50(08), 118-125. DOI: 10.16082/j.cnki.issn.1001-4578.2022.08.017
- [121]She S., Zou X., Zheng X., et al. (2025). Measurement of permeability and radius for asymmetric cylinders with double coils using a simplified analytical model of eddy current testing [EB/OL]. [https://papers.ssrn.com/sol3/papers.cfm?abstract\\_id=5191617](https://papers.ssrn.com/sol3/papers.cfm?abstract_id=5191617).
- [122]Wu X., Zhang Q., Shen G. (2016). Review on advances in pulsed eddy current nondestructive testing technology [J]. *Chinese Journal of Scientific Instrument* , 37(08), 1698-1712. DOI: 10.3969/j.issn.0254-3087.2016.08.003
- [123]She S., Chen Y., He Y., et al. (2021). Optimal design of remote field eddy current testing probe for ferromagnetic pipeline inspection [J]. *Measurement* , 168, 108306. DOI: 10.1016/j.measurement.2020.108306
- [124]Xu Z., Xiao Q. (2019). Outside inspection and quantitative evaluation of pipe defects based on pulsed remote field eddy currents [J]. *Journal of Electronic Measurement and Instrumentation* , 33(02), 80-87. DOI: 10.13382/j.jemi.B1801817
- [125]Yuan X., Li W., Zhao J., et al. (2024). *Novel phase reversal feature for inspection of cracks using multi-frequency alternating current field measurement technique* [M]//Recent Development of Alternating Current Field Measurement Combine with New Technology. Singapore: Springer Nature Singapore, 77-97.
- [126]Yu Z., Tian G., Gao B., et al. (2025). Remote focus field electromagnetic sensing diagnostic system for nondestructive testing [J]. *IEEE Transactions on Instrumentation and Measurement* , 74, 6008613 DOI: 10.1109/TIM.2025.3576956
- [127]Yang L., Zheng W., Gao S., et al. (2020). Steel plate crack defect detection method based on balanced electromagnetic technology [J]. *Chinese Journal of Scientific Instrument* , 41(10), 196-203. DOI: 10.19650/j.cnki.cjsi.J2006769
- [128]Yang L., Zheng W., Li J., et al. (2021). Full-angle detection

- method of pipeline crack based on balanced electromagnetic technology [J]. *Chinese Journal of Scientific Instrument* , 42 (6), 103-112. DOI: 10.19650/j.cnki.cjsi.J2107735
- [129]Zheng W., Yang L., Li J., et al. (2022). Research on synchronous data acquisition and control system of balanced electromagnetic detection technology [J]. *Instrument Technique and Sensor* , (02), 107-111+115. DOI: 10.3969/j.issn.1002-1841.2022.02.022
- [130]Zheng W., Yang L., Li J., et al. (2022). Research on series resonance excitation circuit of pipeline balance electromagnetic internal detection technology [J]. *Instrument Technique and Sensor* , (01), 33-37+48. DOI: 10.3969/j.issn.1002-1841.2022.01.006
- [131]Xiao Q., Feng J., Wang G., et al. (n. d.). Multi-frequency balanced electromagnetic technology for detecting internal and external defects and identifying full-angle surface cracks [J/OL]. *Proceedings of the CSEE* , 1-10. DOI: 10.13334/j.0258-8013.psee.220377.
- [132]Herbert W., Gerhard K., Thomas M. (2016). Recent advancements in ultrasonic in-line inspection [C]//11th Pipeline Technology Conference. Berlin, Germany: PPIM.
- [133]Rosen Group. In-line inspection services for corrosion [EB/OL]. <https://www.rosen-group.com/en/expertise/product-and-service-finder/in-line-inspection-services-for-corrosion#ro-corr-utwm-service>.
- [134]Rosen Group. In-line crack detection, sizing and analysis [EB/OL]. <https://www.rosen-group.com/en/expertise/product-and-service-finder/in-line-inspection-services-for-cracking#ro-cd-ut-a-service>.
- [135]Rosen Group. In-line crack detection, sizing and analysis [EB/OL]. <https://www.rosen-group.com/en/expertise/product-and-service-finder/in-line-inspection-services-for-cracking#ro-cd-ut-c-service>.
- [136]NDT Global. Ndt global introduces evo series 1.0 ultrasonic inline inspection [EB/OL]. <https://www.ndt.org/news.asp?ObjectID=56418>.
- [137]Pipecare Group. Ultrasonic inspection (UT). pipes inspection services [EB/OL]. <https://www.pipe-caregroup.com/ultrasonic-inspection/>.
- [138]Shenyang Lujie Pipeline Technology Co., Ltd. Pipeline corrosion ultrasonic internal detection equipment [EB/OL]. <https://www.syljgd.com/product/guan-dao-fu-shi-chao-sheng-nei-jian-ce-she-bei/>.
- [139]Stephan T., Amanda K., Steven B. (2016). A case study: how latest enhancements in ultrasonic wall measurement ILI technology benefit engineering criticality assessments [C]//Pigging and Integrity Management Conference 2016. Houston, Texas, USA: PPIM.
- [140]Yin S., Zhang H., Shi F., et al. (2025). Bendable phased-array ultrasound transducer for imaging on curved surfaces [J]. *ACS Nano* , 19(8), 8030-8039. DOI: 10.1021/acsnano.4c16028
- [141]Yang H., Wu J., Xia H., et al. (2024). Optimization and system design of piezoelectric ultrasonic sh guided wave method in pipeline wall thickness measurement [J]. *Journal of Applied Acoustics* , 5. DOI: 10.11684/j.issn.1000-310X.2024.05.020.
- [142]Zeng Z., Gao M., Ng C. T., et al. (2023). Guided wave-based characterisation of cracks in pipes utilising approximate bayesian computation [J]. *Thin-Walled Structures* , 192, 111138. DOI: 10.1016/j.tws.2023.111138
- [143]Baker Hughes. PII services overview [EB/OL]. [https://www.bakerhughes.com/sites/bakerhughes/files/2021-12/160122%20PII%20Pipeline%20Solutionsv2%20\(1\).docx\\_0.pdf](https://www.bakerhughes.com/sites/bakerhughes/files/2021-12/160122%20PII%20Pipeline%20Solutionsv2%20(1).docx_0.pdf).
- [144]Rosen Group. In-line crack detection, sizing and analysis [EB/OL]. <https://www.rosen-group.com/en/expertise/product-and-service-finder/in-line-inspection-services-for-cracking#ro-cd-emat-c-service>.
- [145]Rosen Group. In-line crack detection, sizing and analysis [EB/OL]. <https://www.rosen-group.com/en/expertise/product-and-service-finder/in-line-inspection-services-for-cracking#ro-cd-emat-c-ultra-service>.
- [146]Pipecare Group. Electromagnetic acoustic transducer (EMAT): pipeline inspection [EB/OL]. <https://www.pipecaregroup.com/emat-inspection/>.
- [147]Zang Y., Jin Y., Chen C., et al. (2015). Design of mechanical structure of crack detector for pipeline based on the magnetostrictive effect [J]. *Oil & Gas Storage and Transportation* , 34(07), 775-778. DOI: 10.6047/j.issn.1000-8241.2015.07.020
- [148]Trushkevych O., Edwards R. S. (2019). Characterisation of small defects using miniaturised EMAT system [J]. *NDT & E International* , 107, 102140. DOI: 10.1016/j.ndteint.2019.102140
- [149]Rieger K., Erni D., Rueter D. (2020). A compact and powerful EMAT design for contactless detection of inhomogeneities inside the liquid volume of metallic tanks [J]. *tm - Technisches Messen* , 87(5), 349-359. DOI: 10.1515/teme-2019-0124
- [150]Suresh N., Balasubramaniam K. (2020). Quantifying the lowest remnant thickness using a novel broadband wavelength and frequency EMAT utilizing the cut-off property of guided waves [J]. *NDT & E International* , 116, 102313. DOI: 10.1016/j.ndteint.2020.102313
- [151]Takishita T., Ashida K., Nakamura N., et al. (2015). Development of shear-vertical-wave point-focusing electromagnetic acoustic transducer [J]. *Japanese Journal of Applied Physics* , 54(7), 07HC04. DOI: 10.7567/JJAP.54.07HC04
- [152]Thring C. B., Fan Y., Edwards R. S. (2017). Multi-coil focused EMAT for characterisation of surface-breaking defects of arbitrary orientation [J]. *NDT and E International* , 88, 1-7. DOI: 10.1016/j.ndteint.2017.02.005
- [153]Thring C. B., Fan Y., Edwards R. S. (2016). Focused rayleigh wave EMAT for characterisation of surface breaking defects [J]. *NDT and E International* , 81, 20-27. DOI: 10.1016/j.ndteint.2016.03.002
- [154]Lee J. K., Kim H. W., Kim Y. Y. (2013). Omnidirectional lamb waves by axisymmetrically configured magnetostrictive

- patch transducer [J]. *IEEE Transactions on Ultrasonics, Ferroelectrics, and Frequency Control* , 60(9), 1928-1934. DOI: 10.1109/TUFFC.2013.2777
- [155]Lee J. K., Kim Y. Y. (2016). Tuned double-coil EMATs for omnidirectional symmetric mode lamb wave generation [J]. *NDT and E International* , 83, 38-47. DOI: 10.1016/j.ndteint.2016.06.001
- [156]Zhang Y., Huang S., Wang S., et al. (2016). Direction-controllable electromagnetic acoustic transducer for SH waves in steel plate based on magnetostriction [J]. *Progress in Electromagnetics Research M* , 50, 151-160. DOI: 10.2528/PIERM16072203
- [157]Huang S., Sun H., Peng L., et al. (2021). Defect detection and identification of point-focusing shear-horizontal EMAT for plate inspection [J]. *IEEE Transactions on Instrumentation and Measurement* , 70, 1-9. DOI: 10.1109/TIM.2021.3062421
- [158]Zhou H., Tu J., Shen X., et al. (2025). A new dual AC magnetostrictive shear horizontal guided wave transducer [J]. *IEEE Transactions on Instrumentation and Measurement* . DOI: 10.1109/TIM.2025.3593310
- [159]Cen X., Pan G., Wang X., et al. (2021). Optimal design and experimental study of shear wave thickness measuring electromagnetic ultrasonic transducer [J]. *Electronic Measurement Technology* , 44(05), 176-182. DOI: 10.19651/j.cnki.emt.2105672
- [160]Guo Z., Li S., He H., et al. (2021). Research on single mode excitation method of lamb wave based on electromagnetic ultrasonic transducer [J]. *Chinese Journal of Scientific Instrument* , 42(05), 253-260. DOI: 10.19650/j.cnki.cjsi.J2107353
- [161]Sun Z., Li Y., Yang J., Zhai G. (2017). Thickness gauging equipment for ILI of pipelines using EMATs [J]. *China Measurement & Test* , 43(02), 69-72. DOI: 10.11857/j.issn.1674-5124.2017.02.014
- [162]Tang Z., Sun X., Zhang P., et al. (2020). Research on composite electromagnetic ultrasonic transducer integrating thickness measurement and guided wave detection [J]. *Chinese Journal of Scientific Instrument* , 41(09), 98-109. DOI: 10.19650/j.cnki.cjsi.J2006440
- [163]Zhai G., Liang B., Deng C., et al. (2021). Design of high temperature resistant electromagnetic acoustic transducer with double coil structure [J]. *Proceedings of the CSEE* , 41(11), 3943-3951. DOI: 10.13334/j.0258-8013.pcsee.201233
- [164]He J., Xu K., Ren W. (2017). EMAT design of self-excitation with coils and its characteristics study [J]. *Journal of Mechanical Engineering* , 53(16), 134-140. DOI: 10.3901/JME.2017.16.134
- [165]Si D., Gao B., Guo W., et al. (2019). Variational mode decomposition linked wavelet method for EMAT denoise with large lift-off effect [J]. *NDT & E International* , 107, 102149. DOI: 10.1016/j.ndteint.2019.102149
- [166]Suñol F., Ochoa A. D., Garcia E. J. (2019). High-precision time-of-flight determination algorithm for ultrasonic flow measurement [J]. *IEEE Transactions on Instrumentation and Measurement* , 68(8), 2724-2732. DOI: 10.1109/TIM.2018.2869263
- [167]Yacef N., Bouden T., Grimes M. (2019). Accurate ultrasonic measurement technique for crack sizing using envelope detection and differential evolution [J]. *NDT and E International* , 102, 161-168. DOI: 10.1016/j.ndteint.2018.11.018
- [168]Fang Z., Su R., Hu L., et al. (2021). A simple and easy-implemented time-of-flight determination method for liquid ultrasonic flow meters based on ultrasonic signal onset detection and multiple-zero-crossing technique [J]. *Measurement* , 168, 108398. DOI: 10.1016/j.measurement.2020.108398
- [169]Jiao Y., Li Z., Zhu J., et al. (2022). ABIDE: A novel scheme for ultrasonic echo estimation by combining ceemdsswt method with EM algorithm [J]. *Sustainability* , 14(4), 1960. DOI: 10.3390/su14041960
- [170]Zhao S., Zhou J., Liu Y., et al. (2022). Application of adaptive filtering based on variational mode decomposition for high temperature electromagnetic acoustic transducer denoising [J]. *Sensors* , 22(18), 7042. DOI: 10.3390/s22187042
- [171]Faysal A., Ngui W. K., Lim M. H., et al. (2021). Noise eliminated ensemble empirical mode decomposition for bearing fault diagnosis [J]. *Journal of Vibration Engineering & Technologies* , 9(8), 1-17. DOI: 10.1007/s42417-021-00358-y